Quaternary International 322-323 (2014) 78–94

Contents lists available at ScienceDirect

Quaternary International

journal homepage: www.elsevier.com/locate/quaint

Reconstruction of a Pleistocene paleocatena using micromorphology and geochemistry of lake margin paleo-Vertisols, Olduvai Gorge, Tanzania

Emily J. Beverly [a,b,*], Gail M. Ashley [a], Steven G. Driese [b]

[a] Earth and Planetary Sciences, Rutgers University, 610 Taylor Road, Piscataway, NJ 08854-8066, USA
[b] Department of Geology, Baylor University, One Bear Place, Waco, TX 76798-7354, USA

ARTICLE INFO

Article history:
Available online 25 October 2013

ABSTRACT

Olduvai Gorge, Tanzania contains a rich record of Pleistocene paleoclimate and paleoenvironment, as well as an abundance of paleontological and archaeological data. The 2.2 Ma of volcaniclastic infill can be divided into time-slices using dated tuffs. Sediments were deposited in a semi-arid, closed rift basin containing a shallow saline–alkaline lake until ~1.75 Ma. Four trenches in uppermost Bed I sample a ~20 ka time-slice between Ng'eju Tuff (base, 1.818 ± 0.006 Ma) and Tuff IF (top, 1.803 ± 0.002 Ma). They form a ~1 km transect of the lake margin flat that contains both stacked and cumulative paleosols that are interpreted as a heterogeneous paleocatena. Closer to the lake, paleosols are thinner, vertically stacked, and separated by thin tuffs or tufa. Further from the lake margin, there is additional volcaniclastic input, and paleosols are thicker and cumulative. Macroscale and micromorphological features identify these clay-rich paleosols as paleo-Vertisols. Abundant pedogenic slickensides and a variety of ped shapes were observed in the field, as well as micro-ped structures and stress cutans in thin section. Although weakly developed, these paleo-Vertisols also have distinct horizons defined by soil color changes, differing ped shapes, and bulk geochemistry and are indicative of monsoonal precipitation seasonality.

Paleosols and parent materials were analyzed for bulk geochemistry of major, rare, and trace elements. Geochemical proxies reveal changing hydrology not definitively identifiable in the field or micromorphology. Molecular weathering ratios show increased weathering, and mass-balance calculations indicate greater translocations (positive and negative) through time. Lower soil moisture due to a drier climate likely created better-drained conditions allowing for increased pedogenesis. The records of FeMn oxides and zeolites precipitated in rhizoliths are further evidence for changing redox conditions and water chemistry. Redox-sensitive elements such as Fe and Mn were mobilized during saturated soil conditions and precipitated during drier conditions. As the hydrology changed due to increased aridity, zeolites precipitated as rhizoliths due to capillary rise and evaporative pumping of saline–alkaline water. The fluctuating hydrology identified in the paleo-Vertisols deposited between 1.79 and 1.81 Ma is indicative of a precession cycle and consistent with records from Olduvai Gorge and throughout East Africa. This 20 ka time-slice of the 2 Ma drying trend identified in Africa coincides with the first hominin migrations out of Africa at ~1.8 Ma and suggests that hominins were living in a water-stressed environment with annual precipitation seasonality and large variations in precipitation due to precession.

1. Introduction

Previous research has demonstrated that the Pleistocene sediments of Olduvai Gorge, Tanzania contain a rich record of the paleolandscape and an abundance of paleontological and archaeological data. The 2.2 Ma of volcanic and fluvio-lacustrine infill can be divided into chronostratigraphic units using dated tuffs (Gromme and Hay, 1971; Berggren et al., 1995; Tamrat et al., 1995; McHenry, 2004, 2005; Deino, 2012). These units are referred to as time-slices and have been used to reconstruct the paleoenvironment and paleoclimate of the basin (e.g. Ashley and Driese, 2000; Hay and Kyser, 2001; Deocampo et al., 2002; Sikes and Ashley, 2007; Ashley et al., 2009, 2010a, 2010b, 2010c; Barboni et al.,

* Corresponding author. Department of Geology, Baylor University, One Bear Place #97354, Waco, TX 76798-7354, USA.
E-mail address: Emily_Beverly@Baylor.edu (E.J. Beverly).

1040-6182/$ – see front matter © 2013 Elsevier Ltd and INQUA. All rights reserved.
http://dx.doi.org/10.1016/j.quaint.2013.10.005

2010). The Olduvai Gorge Basin is located on the western margin of the East African Rift where incision during the Late Pleistocene exposed 100 m of basin infill (Fig. 1A; Hay, 1976). The sediments were deposited in a semi-arid, closed rift basin containing a shallow saline–alkaline lake, which is inferred to have expanded and contracted with changes in orbital insolation variability until ~1.75 Ma (Kappelman, 1986; Hay and Kyser, 2001; Ashley and Hay, 2002; Ashley, 2007; Magill et al., 2012a, 2012b). The sediments are well exposed and beds can be physically traced, making Olduvai Gorge an ideal locality to study paleosols in a paleolandscape context. Hay (1976) and Leakey (1971) mention numerous pedogenically modified beds found throughout the Olduvai stratigraphy,

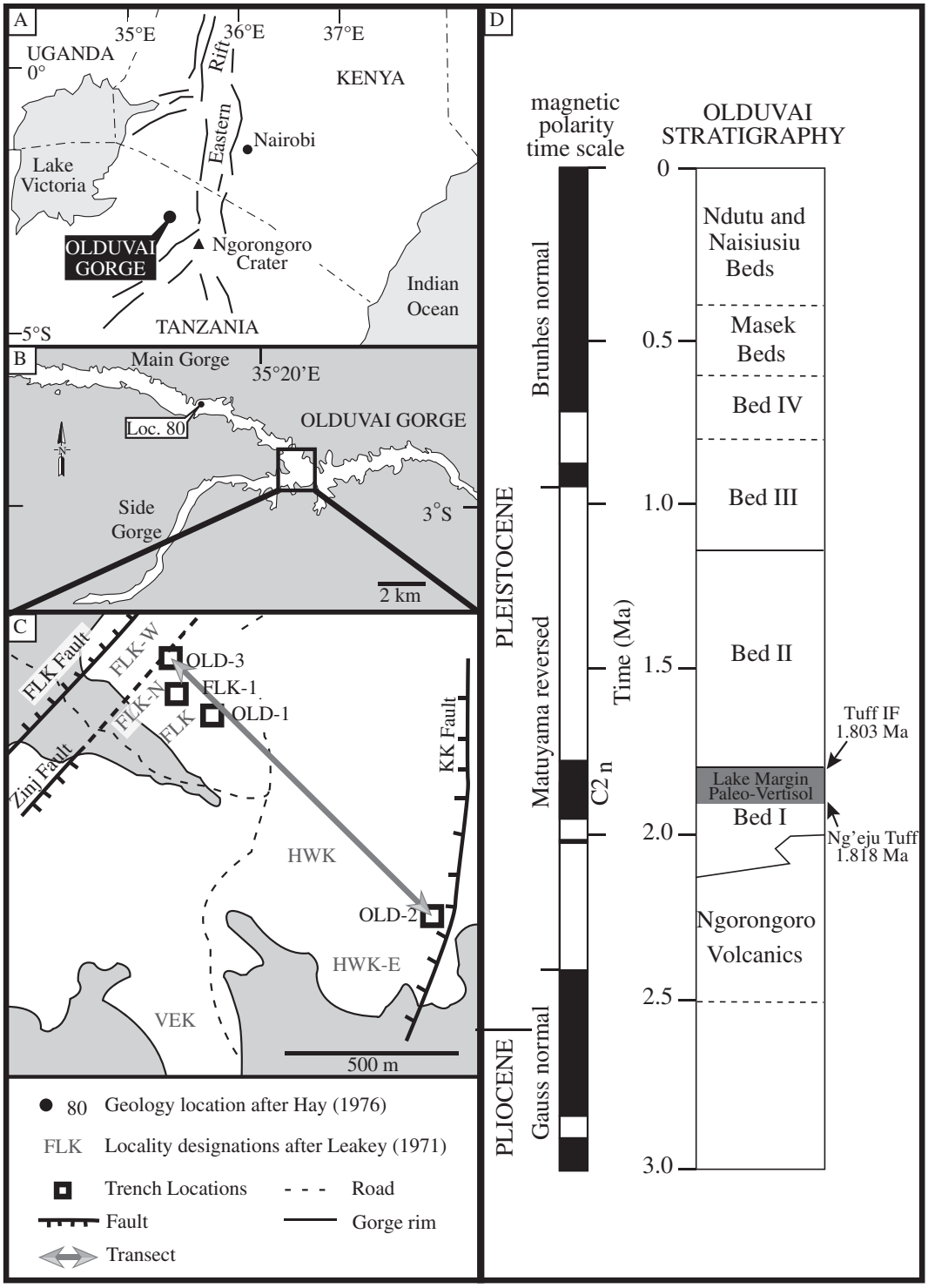

Fig. 1. Location and stratigraphy of Olduvai Gorge, Tanzania. (A) Location of Olduvai Gorge in relation to the East African Rift System. (B) Map of the "junction" where the Main and Side gorges converge and the location of samples collected from paleo Lake Olduvai to the west. (C) More detailed map of junction area indicating of key archaeological sites after Leakey (1971), and the transect and geological sites used in this study. Modified from Ashley et al. (2010a). (D) Pleistocene magnetic polarity time scale adjacent to the Olduvai Basin stratigraphy with the time-slice for this study shown in gray. Modified from Hay (1976).

but few paleosols within the 100 m thick sediment package have been studied in high-resolution. Paleosols are increasingly being recognized as an important aspect of terrestrial environments because soils form at the surface where they directly interact with organisms, atmosphere, and climate. Recent research has combined qualitative descriptions using modern soils as analogs and quantitative proxies using clay mineralogy and whole rock and isotopic geochemistry (Sheldon and Tabor, 2009, and references therein).

Olduvai Gorge is a classic locality for hominins, associated cultural material, and faunal remains. In upper Bed I, the focus of this research, two species of hominin were living near paleo Lake Olduvai: 1) *Homo habilis*, an ancestor of modern *Homo sapiens*, and 2) the now extinct *Paranthropus bosei* (Leakey, 1971; Domínguez-Rodrigo et al., 2007). Most of the archaeological sites are located on the eastern lake margin in the "junction" between the Main and Side Gorges (Leakey, 1971; Hay, 1976) where there is a lack of detailed paleosol research (Fig. 1B). Previous research on paleosols has focused on the isotopic composition of pedogenic carbonates from throughout the Gorge (Cerling and Hay, 1986). More recently research has focused on the calcium carbonate rich Aridisols forming on the well-drained fluvial environment west of paleo Lake Olduvai (Sikes and Ashley, 2007) and red Andisols forming on the volcaniclastic alluvial fan on the eastern margin of the basin (Fig. 2; Ashley and Driese, 2000).

Here, new data are presented from paleosols identified along the eastern margin of paleo Lake Olduvai, Tanzania. This research focuses on a 20 ka time-slice in uppermost Bed I (~1.8 Ma) where the lake periodically flooded and deposited sediment that was subsequently pedogenically modified (Fig. 1C). The time-slice is defined by Ng'eju Tuff (base, 1.818 ± 0.006 Ma) and Tuff IF (top, 1.803 ± 0.002 Ma) and contains both stacked and cumulative paleosols (Deino, 2012). This time-slice correlates with archaeological levels 1–9 from FLK-N where there is the densest concentration of artifacts and large mammal bones (Leakey, 1971; Domínguez-Rodrigo et al., 2007, 2010; Bunn et al., 2010; Ashley et al., 2014a). Upper Bed I also coincides with the time of first migrations of genus *Homo* out of Africa at ~1.8 Ma. The earliest evidence for genus *Homo* outside of Africa appears at the Dmanisi site in Georgia between 1.85 and 1.77 Ma (Gabunia et al., 2000; Lordkipanidze et al., 2007; Ferring et al., 2011). Interpretation of FLK-N has been highly controversial, and a high-resolution study of this time-slice from 1.79 to 1.81 Ma where genus *Homo* was living may lead to a better understanding of the reasons for this migration.

The objectives of this study are to 1) use field description, micromorphology of paleosols, and bulk geochemistry (specifically constitutive mass-balance calculations) to characterize the soil-forming processes and reconstruct the paleoenvironment and paleoclimate, 2) integrate the paleocatena forming on the eastern lake margin within the overall paleolandscape of the Olduvai Basin, and 3) use stacked paleosols to interpret climate change over a ~20 ka time-slice coinciding with the first migrations out of Africa at ~1.8 Ma.

2. Setting

2.1. Geologic setting

Olduvai Gorge is located on the western margin of the East Africa (Gregory) Rift in northern Tanzania (Fig. 1A; Hay, 1976). The Olduvai basin was infilled with volcanics and volcaniclastics beginning at ~2.2 Ma, and a playa lake formed in the center of the basin (Hay, 1976; Hay and Kyser, 2001). The Pleistocene deposits are divided into six units, from Bed I to the Ndutu Beds, and are composed of fluvio-lacustrine sediments interbedded with tuffs (Fig. 1B; Hay, 1976; Ashley and Hay, 2002). The basin-wide stratigraphy of Olduvai Gorge has been previously determined using paleomagnetic epochs (Gromme and Hay, 1971; Tamrat et al., 1995), field mapping (Hay, 1976), mineral chemistry (McHenry, 2004, 2005; Mollel et al., 2009), and $^{40}Ar/^{39}Ar$ dating (Hay, 1992; Deino, 2012). Paleo Lake

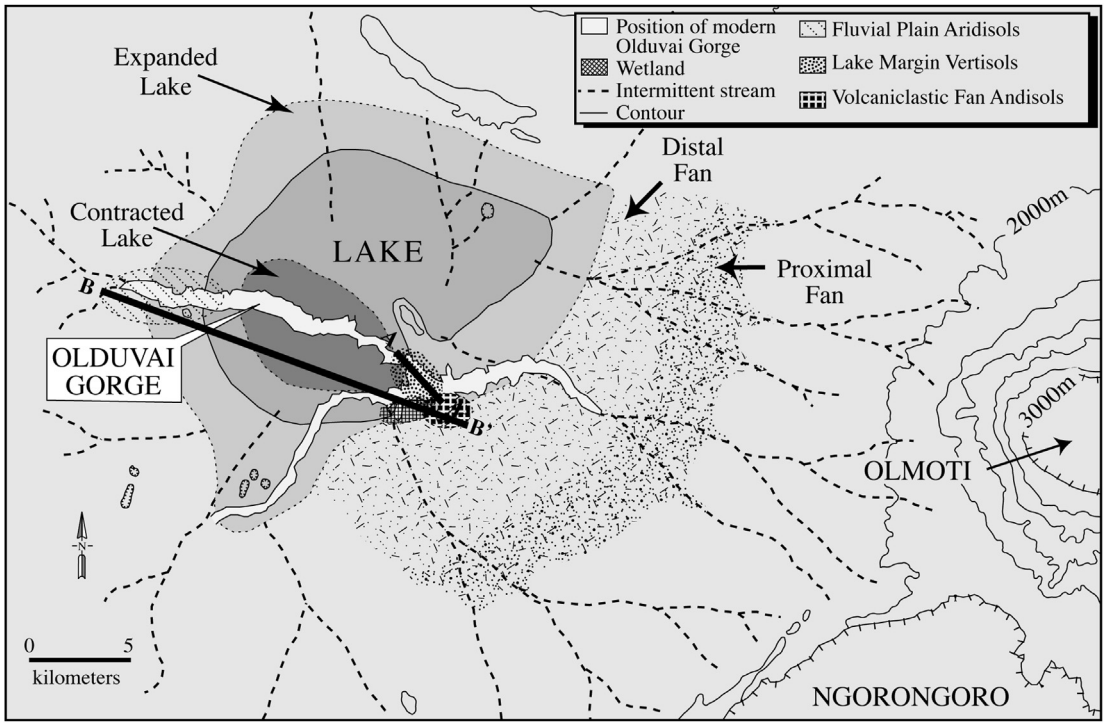

Fig. 2. Paleogeographic map of Olduvai Gorge. Distribution of paleoenvironments, the expansion and compaction of paleo Lake Olduvai during the Pleistocene, and the distribution of soil forming environments are indicated. Two diagrammatic reconstructions are indicated and are shown in Fig. 8. Modified from Ashley et al. (2010c).

Olduvai was the major feature on the landscape between 1.92 and 1.70 Ma and is recorded in Beds I and lowermost Bed II (Hay, 1976; Hay and Kyser, 2001). The hydrologically closed system covered an area of approximately 3500 km^2, draining into paleo Lake Olduvai (Ashley and Hay, 2002). Clay mineralogical analysis determined that this was a non-potable saline–alkaline lake (Hay and Kyser, 2001; Hover and Ashley, 2003; Deocampo et al., 2009). The lake was bounded to the south and east by the Ngorongoro Volcanic Complex (NVC), a group of at least seven volcanoes within the East African Rift, and bounded to the north and west by Precambrian igneous and metamorphic basement. Minor changes in precipitation and runoff resulted in substantial changes in lake area and depth with a low gradient lake floor (Hay, 1976).

The volcanic sources in the nearby NVC deposited an abundance of tuffs in the Olduvai basin allowing for accurate time constraints and enabling high-resolution reconstructions of the environment (e.g. Ashley and Driese, 2000; Hay and Kyser, 2001; Deocampo et al., 2002; Sikes and Ashley, 2007; Ashley et al., 2009, 2010a, 2010b, 2010c; Barboni et al., 2010). This research is focused on a 2–2.5 m thick time-slice of uppermost Bed I between the Ng'eju Tuff and Tuff IF, the boundary that divides Beds I and II (Figs. 1D and 3). A multi-component approach using phenocryst composition successfully demonstrated that Tuff IF and Ng'eju Tuff are laterally extensive and distinct "marker" beds throughout Olduvai Gorge (McHenry, 2004, 2005, 2010). New ^{40}Ar/^{39}Ar dates by Deino (2012) gives an age of 1.803 ± 0.002 Ma and the previously undated Ng'eju

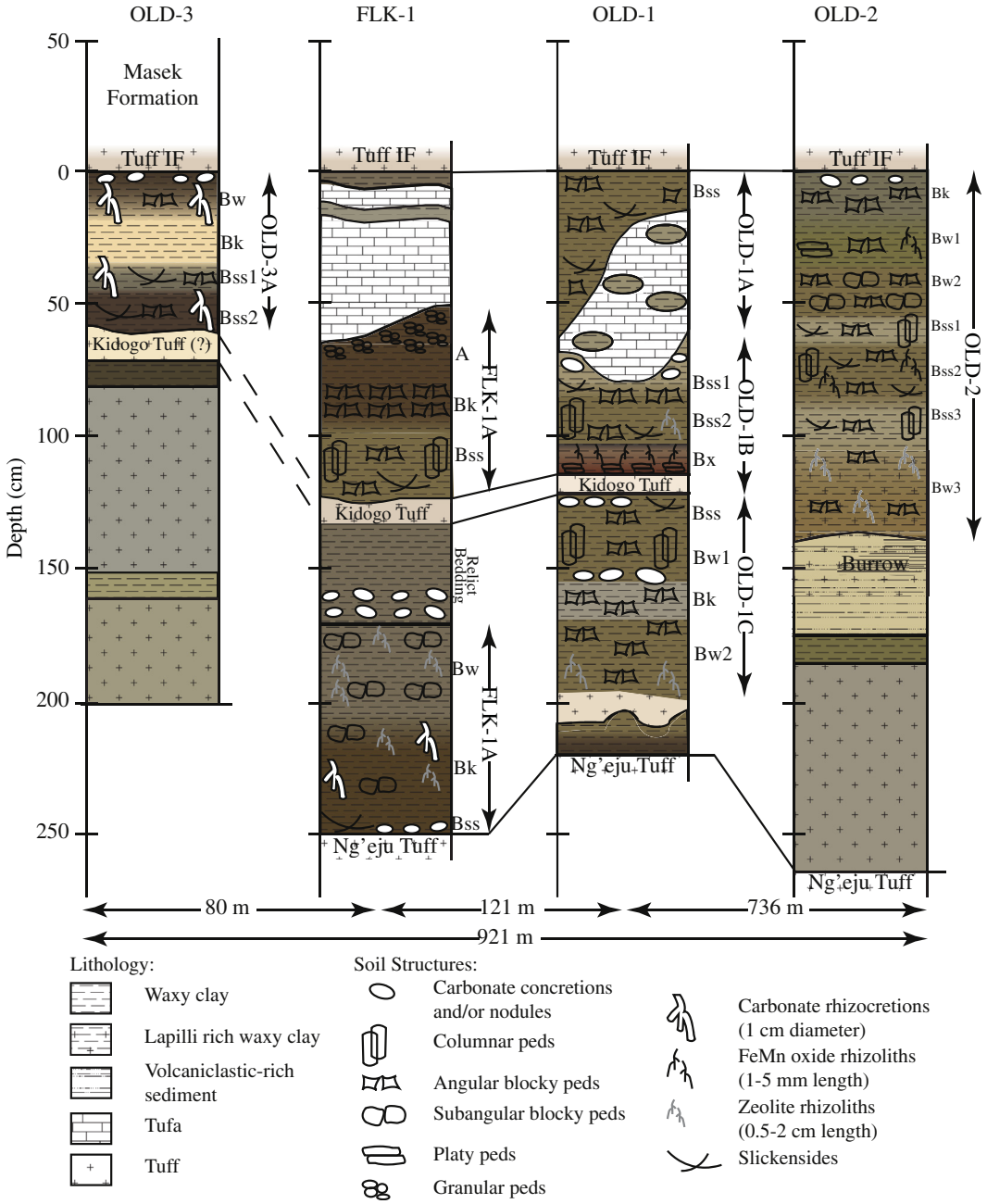

Fig. 3. Stratigraphic correlation of time-slice between Tuff IF and Ng'eju Tuff. Tuff IF is used as a datum, and the four trenches are spread out over ~1 km. Additional correlation made possible using the thin discontinuous Kidogo Tuff (Ashley et al., 2014b). Colors are based on Munsell soil colors and are available in Beverly (2012).

Tuff has an age of 1.818 ± 0.006 Ma (Deino, 2012). This is consistent with the stratigraphy and the paleomagnetic age constraint of 1.785 Ma of the Olduvai subchron (CN2) (Berggren et al., 1995). In addition, using sedimentation rates of 0.1 mm/y and 0.12 mm/y established by Hay (1976) and Ashley (2007), a 2 m thick package of sediment (excluding tuff and tufa beds) would represent ~20 ka interval of time.

2.2. Paleoclimatic and hydrologic setting

The Olduvai Gorge region is a semi-arid environment due to the rain shadow created by the NVC and has an evaporation rate of ~2000–3000 mm/y, which greatly exceeds modern mean annual precipitation (MAP) of 560 mm/y (Hay, 1976; Ashley et al., 2010a). The majority of the precipitation is associated with the West and East African Monsoons during the boreal and austral summers, respectively (Nicholson, 2000). The paleoprecipitation has been estimated to between 500–900 mm/y (Sikes and Ashley, 2007) and 250–750 mm/y (Magill et al., 2012a, 2012b). The mean average temperature for Olduvai Gorge at 3°S is 23 °C and usually varies seasonally by <5 C° (Hay, 1976; Nicholson, 2000).

Multiple proxies have demonstrated that East Africa has experienced a long term drying trend and increased climate variability over the past 2 Ma (Feakins and deMenocal, 2010, and references therein). Stable isotopes of pedogenic carbonates from the Olduvai stratigraphy indicate a general drying trend (Cerling and Hay, 1986; Sikes and Ashley, 2007) as do paleosols in lowermost Bed II (Ashley and Driese, 2000) and marine eolian dust records from northern Africa (deMenocal, 1995). In addition, macrofauna (Plummer and Bishop, 1994; Andrews and Humphrey, 1999), microfauna (Fernandez-Jalvo et al., 1998), and pollen and phytoliths (Bonnefille, 1984; Bamford et al., 2008; Barboni et al., 2010) all show a drying climate through the stratigraphic sequence.

Within the overall drying trend affecting Africa, the Olduvai region was heavily influenced by ~20 ka precession cycles that affect the amount of equatorial solar insolation (Ashley and Hay, 2002; Ashley, 2007; Magill et al., 2012a, 2012b). At the equator, an increase in solar insolation is associated with strengthening of the Northern Hemisphere Monsoons and a generally wetter climate and is often referred to as the orbital monsoon hypothesis (cf. Kutzbach and Liu, 1997; Ruddiman, 2008). This signal is recorded in the lithostratigraphy as the lake periodically expanded and contracted over the broad shallow basin margin depositing continuous beds of waxy clay at intervals consistent with wet periods of a 20 ka precession cycle and earthy claystones forming in lake margin wetlands during dry periods (Hay and Kyser, 2001; Ashley and Hay, 2002; Ashley, 2007). Five complete cycles of lake expansion and contraction are identified from 1.84 to 1.74 Ma and between Tuffs IB and IIA (upper Bed I and lowermost Bed II), and it is inferred that the lake margin sequences reflect precession cyclicity. Evidence for precession cycles is further supported by stable isotopes (Liutkus et al., 2005) and organic carbon from plants (Magill et al., 2012a, 2012b). The data presented here focus on a ~20 ka time-slice ideal for understanding the effects of the precession cycles on the paleoenvironment.

2.3. Previous paleosol research at Olduvai Gorge

Only a few paleosols in upper Bed I and lowermost Bed II have been studied in high-resolution, but Hay (1976) and Leakey (1971) mention numerous pedogenically modified beds found throughout the Olduvai stratigraphy. Early research focused on the isotopic composition of pedogenic carbonates and other terrestrial carbonates (Cerling and Hay, 1986). These carbonates indicate an increase in aridity over the past 2.2 Ma. More recent research has ranged from the study of calcium carbonate-rich silty Aridisols forming in the well-drained fluvial environment of middle to upper Bed I (Sikes and Ashley, 2007) to red Andisols forming in lowermost Bed II on the volcaniclastic alluvial fan (Fig. 2; Ashley and Driese, 2000). These paleosols are summarized in further detail in Ashley et al. (2014a).

2.4. Paleontological, archaeological, and paleoecological records

The focus of this research, upper Bed I, has a high density of artifacts and an abundance of large mammal bones (mostly bovids) clustered around sites FLK, FLK-N, and FLK-NN (Fig. 1C; Leakey, 1971). The time-slice between the Ng'eju Tuff and Tuff IF at FLK-N contains one of the densest concentrations of these materials, but interpretation of this site has been highly controversial (Leakey, 1971; Domínguez-Rodrigo et al., 2007, 2010; Bunn et al., 2010; Ashley et al., 2014b). New data from the time-slice between the Ng'eju Tuff and Tuff IF suggest that a low ridge, approximately 1 m above the surrounding landscape, allowed palms to grow where the soil was better drained, while an abundance of woody plants and sedges grew in the surrounding lowlands, where seepage from groundwater-fed springs provided moisture in a semi-arid climate (Barboni et al., 2010; Ashley et al., 2010a). These new data suggest that the location of the archaeological sites near FLK was a result of the FLK fault and Zinj Fault (related to rifting), which created fault-controlled springs (Fig. 1C). The continued controversy and abundant archaeological record make this time-slice a priority for high-resolution reconstructions of the environment to aid in the interpretation of the site.

3. Methods

3.1. Field methods

Previous research demonstrates that the Ng'eju Tuff (McHenry, 2004, 2005) and Tuff IF (Hay, 1976) are laterally extensive and distinct throughout Olduvai Gorge with 2–4 m of sediment between them. A ~1 km transect was identified in uppermost Bed I, and three locations with known outcrops of the Ng'eju Tuff and Tuff IF were selected for excavation and detailed investigations. These three trenches are designated as OLD-1, OLD-2, and OLD-3 (Figs. 1C and 3). Additional samples and descriptions by GMA in 2007 were used from Trench FLK-1, where previous research had focused on the tufa found beneath Tuff IF (Ashley et al., 2010a, 2010c). These Trenches form a ~1 km cross-section of the lake margin in a NW–SE direction (Fig. 1C). Trench OLD-3 is closest to paleo Lake Olduvai and Trench OLD-2 is almost 1 km away nearest to the alluvial fan at the base of the NVC. Trenches FLK-1 and OLD-1 are located 80 and 201 m, respectively, from Trench OLD-3 (Fig. 3).

All outcrops locations were recorded using GPS, stratigraphy was measured, macroscale features were logged in detail and photographed, and representative samples of each lithology collected. Additional samples for bulk geochemical analysis were collected from the paleosols for calculations of molecular weathering ratios and constitutive mass-balance. Standard geochemical analysis of paleosols requires sampling every 10 cm to determine the geochemical signature of soil horizons (Retallack, 2001). Whole soil clods were also collected at 10 cm intervals for bulk density analysis. Where possible, oriented samples were collected from each soil horizon for thin-section analysis of the micromorphology.

3.2. Laboratory methods

Eighty samples were analyzed for bulk geochemistry. Bulk density (in g/cm^3) of bulk geochemical samples was conducted

using the wax clod method (Blake and Hartge, 1986). After oven drying clods at 60 °C, these samples were pulverized using a mortar and pestle and then sent for commercial analysis to ALS Geochemistry (Reno) for major, rare earth, and trace analyses using a combination of inductively coupled plasma atomic emission spectroscopy (ICP-AES) and inductively coupled plasma mass spectrometry (ICP-MS). Values for bulk density and bulk geochemistry are reported in Beverly (2012) and are available here: http://hdl.rutgers.edu/1782.1/rucore10001600001.ETD.000063988.

All bulk geochemical data from ICP-MS and ICP-AES were converted from ppm to weight % and were applied to molecular weathering ratios (Retallack, 2001). Bulk geochemical data were then evaluated using a constitutive mass-balance approach following Brimhall and Dietrich (1987) and Brimhall et al. (1991a,1991b). Mass-balance models have in the past been used to quantify changes in paleosol chemistry, as opposed to molecular weathering ratios, which can only be used to examine relative changes down profile. Mass-balance is a more powerful tool because it is determined using a parent material and takes into account changes in bulk density.

Possible parent materials were determined following Maynard (1992) using the ratio of TiO_2/Zr of each possible parent material and the ratio of TiO_2 to Zr of the averaged composition of each soil. Deviation from parent material is relatively small in immobile elements like Ti, Al, and Zr. Cross-plots of Zr/(Zr/TiO_2) and TiO_2/(TiO_2/Zr) for each soil and plots of Zr/TiO_2 and TiO_2/Zr versus depth were also used as previous research shows these plots are useful for determining parent material suitability (Ashley and Driese, 2000; Driese et al., 2000).

Nineteen thin sections were commercially prepared by Spectrum Petrographics. Oriented samples were stabilized in the field using Hillquist® Thin Section Epoxy C/D formula. The remaining samples were vacuum-impregnated with epoxy by Spectrum Petrographics prior to thin section preparation. Where possible, thin sections were prepared from each paleosol at both the top and bottom, to determine whether any changes in pedogenic microstructures had occurred down profile. In some cases, fine ped size and damage during transport precluded thin section analyses in every horizon. Thin sections were also prepared from other lithologies sampled within the four trenches including: tufa, tuff, waxy lake clay, and volcaniclastic-rich sediment. Micromorphological analysis was conducted according to soil micromorphological techniques established by Brewer (1976) and Fitzpatrick (1993) using an Olympus BX-51 polarized light microscope equipped with a 12.5 MPx digital camera and ultraviolet (UV) fluorescence attachment (at Baylor University). Abundance of organic content was visually estimated by subjecting the thin section to UV causing the organic matter to autofluoresce. Photomicrographs were taken using three different wavelength filters, Nu, Nb, and TXRED in addition to reflected light, cross-polarized light (XPL), and plane polarized light (PPL) of unique and representative features.

4. Results

The results are organized geographically from northwest to southeast (Fig. 3). Paleosols are all depicted using Tuff IF as a datum for continuity and can be correlated using Tuff IF, Ng'eju Tuff, and the newly defined Kidogo Tuff (Ashley et al., 2014b).

4.1. Field descriptions

Trench OLD-3 is located in FLK North about 7 m from Trench FLK-N-3 referred to in Ashley et al. (Fig. 1C; 2010a). The top 2 m were measured and described but the Ng'eju Tuff was not exposed at this location. One paleosol with four distinct horizons was identified directly beneath Tuff IF (Fig. 3). The paleosol overlies a thin discontinuous tuff, likely the Kidogo Tuff. The paleosol is divided into four horizons: Bw, Bk, Bss1, and Bss2. Pedogenic slickensides can be found in the Bss1 and 2 horizons as well as an abundance of carbonate-filled root traces about 1 cm in diameter and of various lengths 5 cm or less. Beneath the tuff is a 10 cm bed of waxy clay with no evidence of pedogenic modification. Below this thin bed of waxy clay is another 70 cm thick tuff with alternating beds of ash fall and lapilli.

Trench FLK-1 is located in FLK and is 80 m to the southeast of Trench OLD-3 (Fig. 1C). Data regarding the freshwater spring tufa found at this location are presented in Ashley et al. (2010a, 2010b). A total of 2.5 m of sediment containing two paleosols were described between Tuff IF and the Ng'eju Tuff (Fig. 3). The uppermost portion of the Trench consists of 60 cm of tufa with waxy clay intermixed. A paleosol referred to as FLK-1A was identified beneath the thick bed of tufa. FLK-1A is divided into three horizons: an A horizon with granular ped structure, a Bk horizon, and a Bss horizon with pedogenic slickensides on columnar peds. The Kidogo Tuff separates FLK-1A and paleosol FLK-1B. The upper 20 cm are thinly laminated with no physical evidence of pedogenesis and an abundance of carbonate concretions at the base of the relict bedding. The Bw horizon has abundant zeolite-filled root traces and subangular blocky peds, a clear indicator of pedogenesis. The Bk horizon contains both zeolite- and carbonate-filled root traces. Directly above the Ng'eju Tuff, is a Bss horizon with pedogenic slickensides.

Trench OLD-1 is located in Maiko Gully in the "junction" area (Fig. 1C; Hay, 1976). The Trench exposes a 2.2 m thick package of sediment between Ng'eju Tuff and Tuff IF contains 3 distinct paleosols (Fig. 3). These paleosols are designated OLD-1A (upper), OLD-1B (middle), and OLD-1C (lower). Paleosol OLD-1A occurs between Tuff IF, and a large wedge of clean white tufa containing small pockets of clay. OLD-1A ranges from 25 to 50 cm thick and is characterized by pedogenic slickensides and angular blocky peds. This thin paleo-Vertisol contains one Bss horizon. Paleosol OLD-1B is 35 cm thick and occurs between the tufa and Kidogo Tuff. The paleosol can be subdivided into three horizons. The Bss1 horizon contains slickensided angular blocky peds, and the Bss2 horizon contains slickensided columnar peds and zeolitized rhizoliths. The Bx horizon (fragipan) has a distinct dark red color (10R 3/6) and platy peds that restricted roots and are preserved as FeMn oxide rhizoliths (Fig. 4A). Paleosol OLD-1C is a 70 cm thick paleosol that occurs between the Kidogo Tuff and another discontinuous tuff. It has four distinct horizons: Bss, Bw1, Bk and Bw2. The Bss horizon has gilgai and columnar peds with abundant pedogenic slickensides (Fig. 4B). The Bw1 horizon has no distinguishing features, but has angular blocky peds that transition into a Bk horizon. The Bw2 horizon contains an abundance of zeolitized rhizoliths and zeolitized lapilli, which increase in abundance near the base of the paleosol. Beneath the thin discontinuous tuff is a thin 10 cm bed of non-pedogenic waxy clay, which was deposited on top of the Ng'eju Tuff. The bed contains abundant organic material that can be seen in further detail in thin-section.

Trench OLD-2 is located in HWK-E and is 736 m southeast of Trench OLD-1 and almost 1 km from Trench OLD-3 (Fig. 1C). The Trench is 2.65 m deep and contains one cumulative paleosol interval (135 cm thick) directly beneath Tuff IF (Fig. 3). It is likely that two soils formed within this interval one approximately 45 cm thick and another 90 cm thick, but as no complete soil profile can be identified, these paleosols are classified as cumulative. The paleosol has been divided into 7 horizons. The Bk horizon is weakly developed, but the Bw1 horizon has platy and angular blocky peds as well as FeMn rhizoliths and an addition of pyroclastic material. This

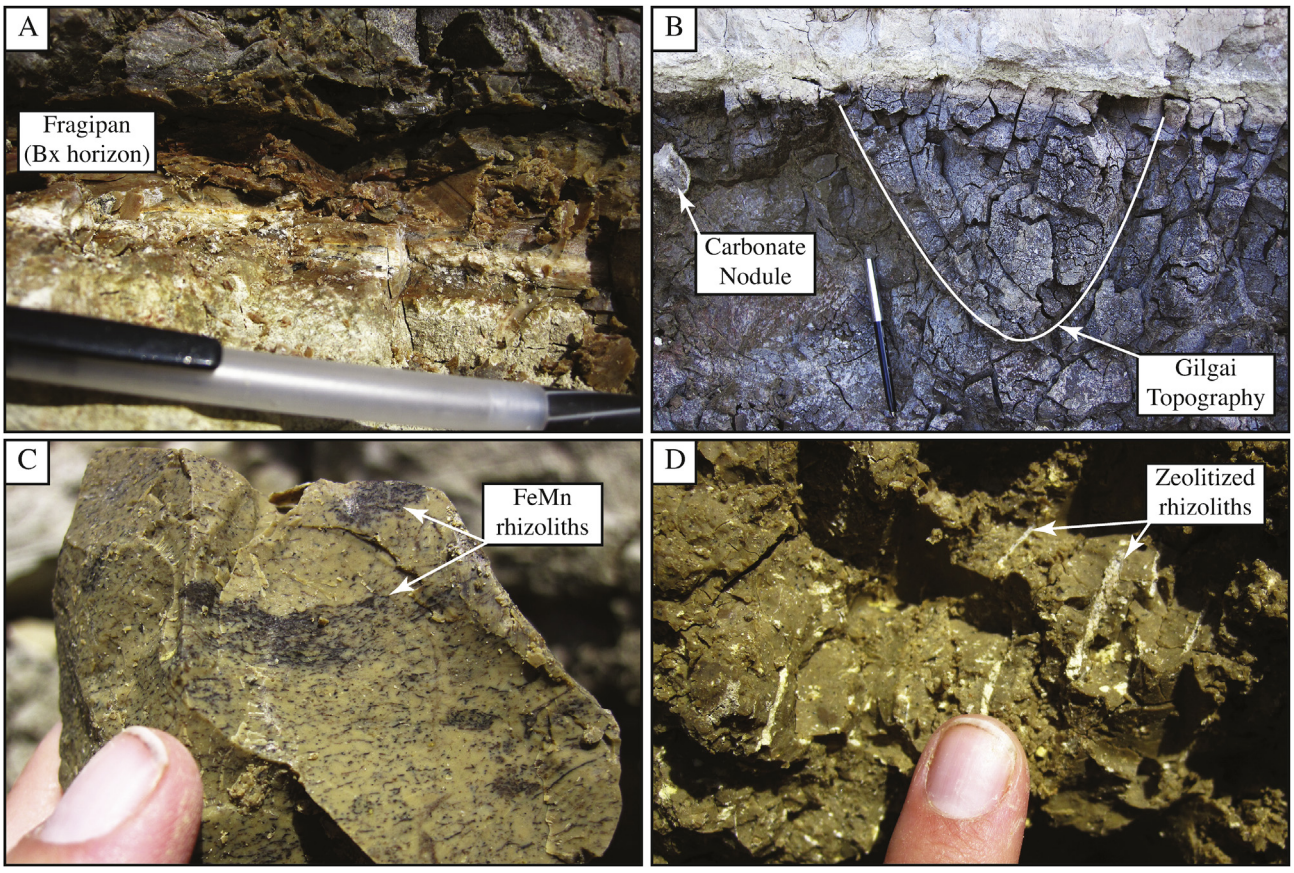

Fig. 4. Field photographs of key pedogenic features. (A) Fragipan in paleosol OLD-1B formed on top of Kidogo Tuff. (B) Gilgai topography outlined in white, typical of a Vertisol from paleosol OLD-1C. (C) FeMn rhizoliths throughout the matrix and concentrated in layers likely from a root mat in the Bss2 horizon of OLD-2A (Ashley et al., 2013c). (D) Zeolitized lapilli and rhizoliths found throughout the Bw3 horizon of OLD-2A.

suggests that this may have been the boundary between two distinct paleosols, but the Bw1 horizon has been welded onto a Bw2 horizon with subangular blocky peds. Pedogenic slickensides are abundant on columnar peds in the Bss1, Bss2, and Bss3 horizons, but the FeMn rhizoliths are highly concentrated in the Bss2 horizon and disappear abruptly below this horizon (Fig. 4C). The Bw3 horizon has an abundance of zeolitized rhizoliths and zeolitized lapilli that increase in abundance with depth (Fig. 4D). Below the paleosol is a 40 cm thick bed of volcaniclastic-rich reworked sediment containing a large burrow. The burrow is a mixture of volcaniclastic sediment and the waxy paleosol clay from above. Beneath the volcaniclastic bed is a thin (12 cm) bed of waxy clay with pedogenic angular blocky peds and slickensides. Under the waxy clay is an 80 cm thick bed of tephra with alternating layers of lapilli and ash fall that directly overlies the Ng'eju Tuff.

4.2. Paleosol micromorphology

Paleosol OLD-3A is volcaniclastic-rich with an irregular blocky micro-ped structure and little organic matter. Zeolitized rhizoliths and lapilli are identified throughout the thin sections (Fig. 5A). Stress cutans are present throughout but are generally weakly developed. Paleosols in Trench FLK-1 have a weak insepic matrix fabric and minimal pyroclastic materials. The paleosol matrix contains an abundance of FeMn oxides and a weak organic signature throughout the horizons, but no other distinguishing features.

Paleosols in Trench OLD-1 generally have greater development of micromorphological features. The matrix of the Bss horizon of the OLD-1B paleosol has an insepic matrix fabric and an irregular blocky micro-ped structure. Grains within the matrix are predominately mafic minerals and are, on average, much smaller than those observed in other paleosols ($\sim$100 μm). The horizon also has an abundance of FeMn oxides in the soil matrix. The top of the fragipan (Bx horizon) is characterized by very little clastic input and by an abundance of FeMn oxide-filled rhizoliths and organic matter. The clay is highly birefringent and oriented parallel to the horizon. The base of the fragipan is similar to the upper section in that the clay is highly birefringent, but organic matter is more distinctly concentrated in layers (Fig. 5B). Paleosol OLD-1C is characterized by a skelsepic matrix fabric and stress cutans surrounding both FeMn oxide-filled rhizoliths, as well as volcaniclastic grains (Fig. 5D). Irregular blocky micro-ped structure formed in OLD-1C with sesquans along the ped boundaries. The thin, non-pedogenic waxy clay present at the base of Trench OLD-1 shows minimal volcaniclastic contributions, and the clay is highly birefringent and oriented parallel to the horizon with an abundance of organic matter.

The micromorphologic features of cumulative paleosol OLD-2A are well developed in comparison to paleosols closer to the lake. The matrix fabric is both weakly insepic and skelsepic with stress cutans surrounding both root traces and grains (Fig. 5E). The Bw1 horizon also shows evidence for a complex history of soil moisture conditions. Root voids were first lined with FeMn oxide and then zeolite crystals (Fig. 5F). Micro-peds have an irregular blocky shape, and little to no organic matter is present (Fig. 5C). The Bss2 horizon also has evidence for a skelsepic fabric with stress cutans surrounding both grains and root traces as well as a generally masepic fabric. This horizon also contains volcaniclastic-rich pedorelicts (Fig. 5G). Although there is no evidence for multiple phases of soil

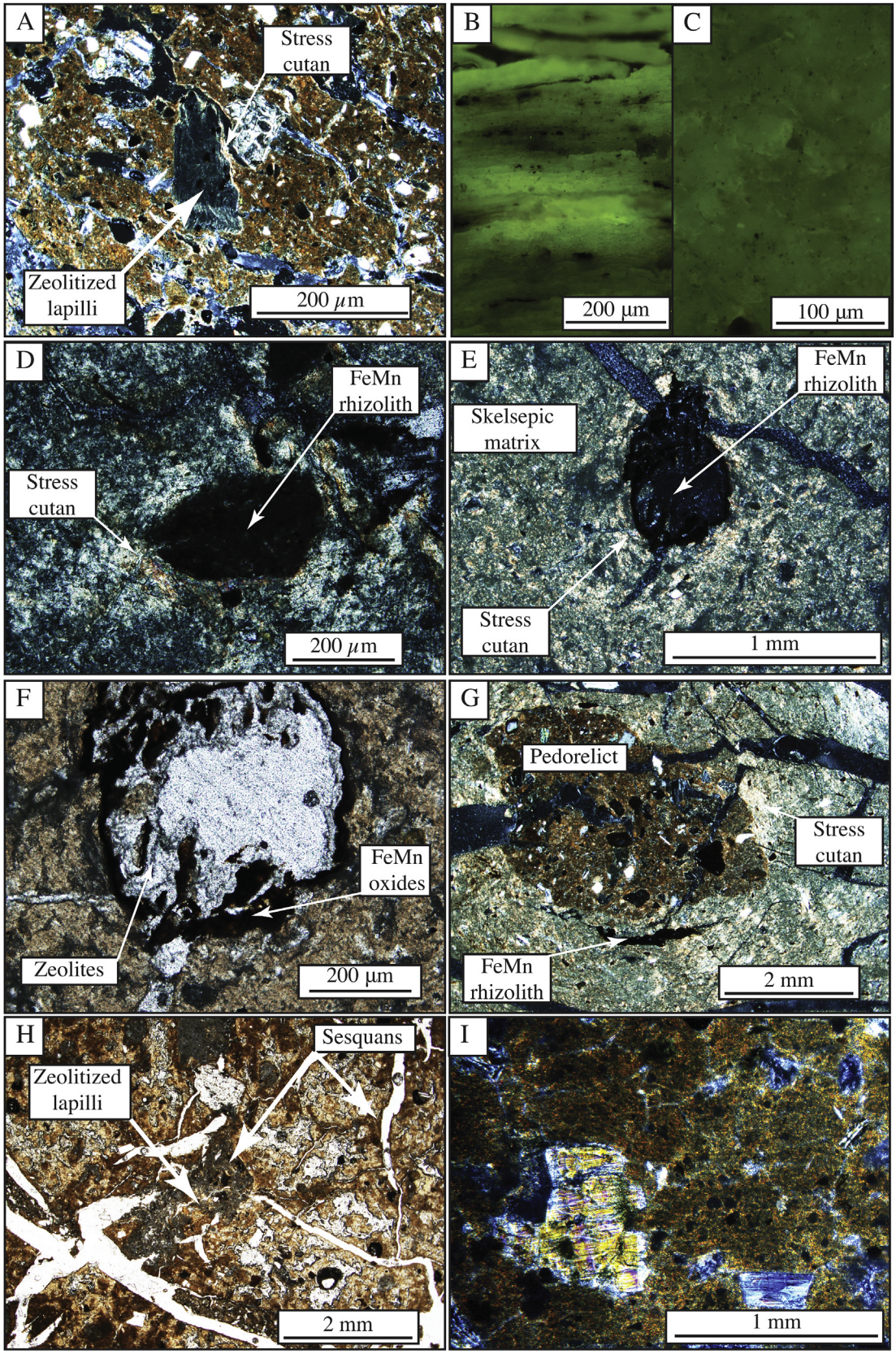

Fig. 5. Photomicrographs of key pedogenic microstructures. (A) Volcaniclastic rich matrix, zeolitized lapilli, and irregular blocky micro-ped structure from the Bw horizon of paleosol OLD-3A; 1.25x XPL. (B) Abundant organic matter visible using UV fluorescence from the fragipan in paleosol OLD-1B; 10x NB Filter. (C) Little to no organic matter autofluorescing in the Bss2 horizon of paleosol OLD-2A; 20x NB Filter. (D) Cross section of FeMn rhizolith with a stress cutan in paleosol OLD-1C that formed as the paleo-Vertisol expanded and contracted aligning the clays; 10x XPL. (E). Stress cutan surrounding a cross section of FeMn rhizolith and an insepic matrix fabric from the Bw1 horizon of paleosol OLD-2A; 4x XPL. (F) Close-up of rhizolith in B with a complex history, first lined with FeMn oxide and zeolites. From the Bw1 horizon of paleosol OLD-2A; 10x PPL. (G) A stress cutan formed around a volcaniclastic-rich pedorelict and a masepic matrix fabric from Bss2 horizon of paleosol OLD-2A; 1.25x XPL. (H) Volcaniclastic-rich matrix with irregular blocky micro-ped structure, sesquans along ped boundaries, and zeolitized lapilli from the Bw3 horizon of paleosol OLD-2A; 10x PPL. (I) Waxy lake clay parent material; 4x XPL.

moisture conditions in this horizon, minerals were precipitated along ped faces with irregular blocky structure. These minerals do not have the characteristic crystal habits of zeolites and may either be carbonate or evaporite precipitates. This horizon contains little to no organic matter. The lowest horizon (Bw3) is very different from the horizons above. The horizon is rich in volcaniclastic material with an insepic matrix fabric, and although stress cutans can be identified, they are less numerous than in the horizons above. Pedorelicts are similar to the surrounding matrix, but are much darker in color. Volcaniclastic grains show evidence of weathering along the grain boundaries and pitting. In addition, sesquans have formed around grains and along ped boundaries in some cases (Fig. 5H). Irregular blocky micro-ped structure is common and in some cases, clay and silt filled in cracks between peds.

Several thin sections from the waxy lake clay were also analyzed for comparison to the paleosols. The samples are from Trench 46 (see Ashley and Driese, 2000) and are slightly younger, but are representative of lake clay found throughout Olduvai Gorge. Fig. 5I illustrates a typical waxy lake clay, which is dominated by clay with varying amounts of unweathered tephra and no microstructures.

4.3. Mass-balance geochemistry

4.3.1. Parent material determination

Parent materials included sediment or tephra above and below each soil, an average of the tuff compositions, and an average of two samples of waxy lake clay from the center of paleo Lake Olduvai from the area referred to as Loc. 80 (Fig. 1C, Hay, 1976). Two Loc. 80 lake samples were analyzed: one from the top and one from the bottom of the time-slice being studied. These serve as references to evaluate any changes in parent material composition due to the fluctuating chemistry, characteristic of a playa lake such as paleo Lake Olduvai. Sample GA-37-99 occurs 10 cm below Tuff IF, and GA-47-99 is 160 cm below Tuff IF. The percent deviation was calculated for all possible parent materials for each soil and is reported in Table 1.

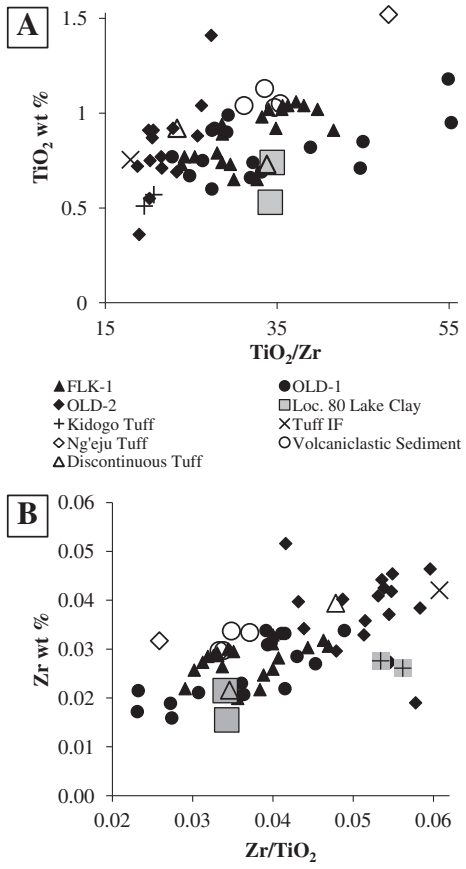

Fig. 6. Parent material determination. (A) TiO_2/Zr vs. wt% TiO_2. (B) Zr/TiO_2 vs. wt% Zr. Both A and B indicate that the waxy lake clay from Loc. 80 is the appropriate parent material for mass-balance calculations as all other potential parent materials above and below the paleosols plot well outside the range of paleosol values. Location of Loc. 80 shown on Fig. 1B.

Table 1
Percent deviation of possible parent materials above and below each paleosol.

Lithology:	OLD-1A	OLD-1B	OLD-1C	OLD-2A	OLD-3A	FLK-1A	FLK-1B
Average Loc. 80 lake clay	−0.3	13.4	−4.8	−36.8	16.8	−13.5	3.8
Kidogo Tuff	–	99.3	−3.3	−7.1	−10.4	43.7	–
Ng'eju Tuff	–	–	–	–	–	–	−25.7
Tuff IF	65.4	966.5	–	20.9	123.4	65.4	–
Volcaniclastic sediment	–	–	–	−35.5	–	–	–

– Indicates parent material not appropriate for paleosol.

Grain size analyses demonstrated that all of the paleosols have 80% or greater clay/silt-sized fractions. This fine grain size is unlikely to have been produced strictly from pedogenesis and therefore the parent material must have been clay-rich. Because of proximity to the paleo lake margin (Fig. 2), this area would have intermittently been flooded, periodically depositing waxy lake clay sediment that then was later pedogenically modified. In addition, paleosols in Trenches OLD-1, OLD-3, and FLK-1 are closer to the composition of lake clay compared to any other potential parent material, and all deviate by less than 17% (Table 2). Other possible parent materials can deviate by up to 900% from the lake clay (Table 1). Suitability of the lake clay parent material can also be demonstrated in cross-plots of TiO_2/Zr vs. weight % of TiO_2 and Zr/TiO_2 vs. weight % Zr (Fig. 6). Generally, the waxy lake clay compositions (gray squares) plot near the center of each paleosol. The waxy lake clay, in general, contains less Ti and Zr than the paleosols, and therefore plots slightly lower than the paleosol samples. Thus, it is the best choice of parent material because the strata above and below are well outside the range of paleosol values.

Table 2
Percent deviation of parent material chosen for each paleosol.

Paleosol	Percent deviation (Ti/Zr)	Parent material
FLK-1A	−13.5	Average Loc. 80 lake clay
FLK-1B	3.8	Average Loc. 80 lake clay
OLD-1A	−0.3	Average Loc. 80 lake clay
OLD-1B	13.4	Average Loc. 80 lake clay
OLD-1C	−4.8	Average Loc. 80 lake clay
OLD-2A	−36.8	Average Loc. 80 lake clay
OLD-3A	16.8	Average Loc. 80 lake clay

In contrast, the paleosol in Trench OLD-2 has a more complicated parent material history, and the percent deviation is much less (−7.1%) in the 40 cm thick tuff above Ng'eju Tuff as compared to the −36.8% deviation in the lake clay (Table 1). The TiO_2/Zr vs. weight % TiO_2 and Zr/TiO_2 vs. weight % Zr cross-plots indicate that this unnamed, discontinuous tuff is geochemically a closer match to the paleosol (Fig. 6). However, the high percentage of clay present within this paleosol makes it unlikely that the tuff is the only parent material source, and it is more likely that the parent material is a

combination of the waxy lake clay and pyroclastic material similar in composition to this tuff. The cumulative paleosol in Trench OLD-2 is paleogeographically furthest from paleo Lake Olduvai (~2 km; Fig. 2) (Hay and Kyser, 2001) and closest to the NVC (McHenry, 2005). This is an ideal location for a parent material characterized by less lake clay contribution and more tephra.

Various combinations of Loc. 80 waxy lake clay (GA-37-99) and the unnamed discontinuous tuff were tested to approximate the composition of the parent material. Further analysis demonstrated that a combination ("model") parent material, which more closely approximated the parent material, was not necessary. Inclusion of such a combination parent material did not significantly change the mass balance results. In most cases, the translocation values were enriched approximately 10% compared to a solely lake clay parent material. This was true except where large translocations occurred, and a combination parent material further exaggerated the already large translocations. Thus, it is clear that using a combination parent material might actually introduce more error into the mass-balance calculations and therefore was not appropriate. As a result, the bulk density and geochemical measurements from the lower waxy lake clay sample (GA-47-99) were used for mass-balance calculations for paleosols OLD-1C and FLK-1B, and the measurements from the upper sample (GA-37-99) were used for calculations for OLD-1A and B, OLD-2A, OLD-3A, and FLK-1A.

4.3.2. Determination of immobile index element

Both Zr and Ti are commonly used as an immobile index element in constitutive mass-balance calculations, and the appropriate immobile index element can be evaluated in several ways (Chadwick et al., 1990; Sheldon and Tabor, 2009, and references therein). First, at Olduvai Gorge, two extraneous sources of Zr are possible: the semi-arid climate allows for the introduction of zircon silt grains in windblown dust, and the easterly trade winds blow volcanic ash containing zircon from the volcaniclastic alluvial fan on the eastern margin of the basin (Fig. 2). Secondly, as determined by Stiles et al. (2003a, 2003b) for Texas Vertisols, the Zr content of is mainly located in the sand and coarser silt-sized fractions of the paleosol, whereas Ti is preferentially located in the <20 μm clay and fine silt-size fractions. The paleo-Vertisols have 80% (or greater) clay/silt content (Beverly, 2012), which makes Ti is the better choice of immobile index element. Finally, if two elements such as Ti and Zr have similar immobility, traditionally the more abundant element is chosen because there is less analytical uncertainty (Sheldon and Tabor, 2009). In these paleosols, Ti is generally about 30 times more abundant than Zr.

4.3.3. Translocation calculations

The results of translocation calculations are grouped into three categories: 1) clay and/or zeolite accumulation, 2) carbonate, and 3) redox-responsive elements. Certain elements react predictably due to biological processes in the soil or during pedogenesis forming minerals (e.g. authigenic clay or zeolites). Translocation of Na, Al, Si, and Mg are grouped together to illustrate any change in smectite clay or Na-zeolite accumulation with depth. Typically, Mg does not react with these elements, but rather with Ca and Sr, which are often indicators for translocation of carbonate. The abundance of Mg-rich smectite in this system obscures any signal associated with carbonate. The redox-sensitive elements (V, Fe, Cu, and Mn) can be important in determining the paleohydrology of the system. Cu is also important in the formation of organic ligands (Brantley et al., 2007), and where Cu deviates from other redox-sensitive elements may be an indicator of biologic activity within the soil.

Mass-balance for paleosol OLD-3 was not included here for simplicity, but can be found in Beverly (2012) and have comparable overall trends to those found in Trench FLK-1. The greatest amount of translocation at Trench FLK occurs in the following order: Na > Al > Si > Mg (Fig. 7A). Paleosol FLK-1A shows general positive translocation with depth in both the clay/zeolite and redox-responsive categories. Paleosol FLK-1B shows a significant enrichment in Na, Mg, Al, and Si near the top of the paleosol, ranging from 25 to 110%. Below this depth both Na and Al show a gradual enrichment, Si shows little change with depth, but Mg continually decreases with depth from 30% to −60%. In paleosol FLK-1A, the redox-responsive elements, Fe, Cu, and V, are depleted at the surface and enriched down profile (Fig. 7B). Cu shows the greatest amount of depletion of −46% and Fe, V, and Cu are all enriched at depth to between 20 and 30%. On average, these elements are more depleted in paleosol FLK-1B, with very little variability down profile. Mn does not correspond to other redox sensitive elements.

Paleosols from FLK-1 also have large depletions of Ca (−80 to −90%), with Sr generally less depleted than Ca (Fig. 7C). Sr is also much less depleted (~−17%) in FLK-1B compared to paleosols in Trenches OLD-1, 2, and 3 as well as paleosol FLK-1A. The mass-balance profiles from paleosols FLK-1A and FLK-1B also show evidence for carbonate accumulation in Bk horizons (Fig. 3). In paleosol FLK-1B, this carbonate is concentrated in rhizoliths.

The three paleosols within Trench OLD-1 have distinct overall trends (Fig. 7D–F). The clay/zeolite accumulation category has the greatest amounts of translocation in this order: Na > Mg > Si > Al (Fig. 7D). In both paleosols OLD-1A and OLD-1B, the majority of the translocation profiles indicate that elements are being retained at the base with some elements showing varying degrees of depletion at the surface. Paleosols OLD-1A and OLD-B also have greater negative and positive translocations than those at OLD-1C, with the exception of Mn. Sr is generally slightly less depleted than Ca, but both elements are generally depleted 90–100% compared to the parent material in all three paleo-Vertisols (Fig. 7F). In OLD-1A, both Sr and Ca are less depleted at depth, but no carbonate enrichment was detectable in the field. OLD-1B contains no enrichments concentrated in a horizon. In OLD-1C, the over 100% enrichment in Sr and ~40% in Ca was detectable in the field and was identified there as a Bk horizon (Fig. 3).

The redox-responsive elements in paleosol OLD-1A indicate depletion from the surface and retention to slight enrichment at the base. OLD-1B has little to no depletion at the surface, but significant gains at the base, especially in V (~160%). In comparison, OLD-1C shows a much more consistent depletion of V (−60%). Cu is similarly depleted on average ~60%, but is ~10% less depleted at the surface. Additionally, greater Fe translocations occur in paleosol OLD-1C. Paleosols OLD-1A and OLD-1B have an average Fe translocation value of −5% and 1%, respectively, whereas paleosol OLD-1C is consistently depleted about −25%.

The translocation profiles from the clay/zeolite accumulation and redox-responsive categories in paleosols FLK-1A, OLD-1A, and OLD-1B (the upper paleosols above the Kidogo Tuff; Fig. 3) generally show more variability within the profile and greater amounts of translocation than the lower paleosols FLK-1B and OLD-1C. This is best illustrated using modified box plots of translocations. Na and Fe are plotted as representative examples (Fig. 8A and B). Both plots show an increase in translocation with an increase in mean (vertical line) and an increase in the range of values from the lower to the upper paleosols.

In the cumulative paleosol from Trench OLD-2, the clay/zeolite accumulation category has the greatest amounts of translocation in this order: Na > Al > Si > Mg (Fig. 7G). These elements are depleted at the surface, ranging from −70% to as little as −16%, but at 25 cm depth Na, Al, Si, and Mg are all enriched over 100%. The remainder of the profile shows a gradual depletion in these elements with depth. The redox-responsive elements, Fe, Cu, V, and Mn also show depletion at the surface with V showing the greatest amounts of

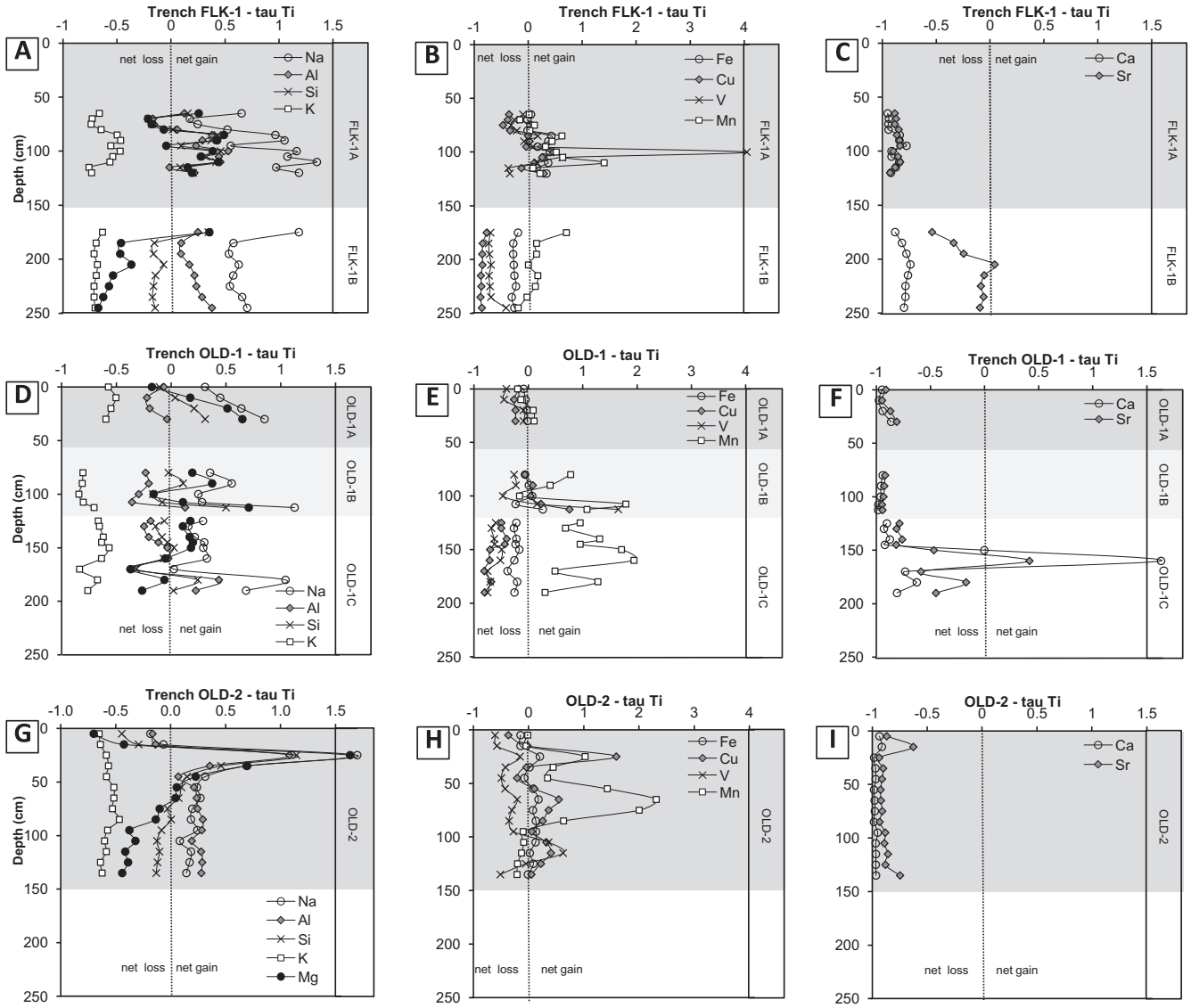

Fig. 7. Constitutive mass-balance calculations. (A–I) Elements grouped according to similar reactions to biological processes or pedogenesis. Ti held constant as the immobile element (Tau Ti) and positive values indicate a net gain and negative values indicate a net loss relative to the parent material. Multiply by 100 to convert to percent gains or losses. (A–C) Na, Al, Si, K, and Mg translocations. (D–F) Ca and Sr translocations. (G–I) Fe, Cu, V, and Mn translocations.

depletion (−60%), and enrichment at 25 cm depth with the greatest translocations in Cu of 160% (Fig. 7H). Sr and Ca are almost consistently depleted between −90 and −100% compared to the parent material (Fig. 7I). Near the surface Ca is slightly less depleted by ~10% and Sr by 30%.

5. Discussion

This ~20 ka time-slice of uppermost Bed I encompasses 4 sites which expose intercalated tuffs, tufa, lake clay, and volcaniclastics on the eastern margin of paleo Lake Olduvai. Most of the sediment has been pedogenically modified with tuffs bracketing these paleo-Vertisols, which allow for correlation and interpretation as a paleocatena as well as paleoclimate. In soil science, a catena is defined as a sequence of soils with similar parent materials and climate, but topography has a significant effect on the development of the soil (Klaus et al., 2005). The paleocatena extends across the lake margin in a NW–SE direction over ~1 km towards the alluvial fan at the base of the NVC (Figs. 1C and 2). The complex history of pedogenesis recorded in this time-slice also gives great insight into a previously unstudied soil-forming environment (i.e. lake margin) and the heterogeneous nature of soil development.

Soil development is traditionally described using 5 soil-forming factors: climate, organisms, topography, parent material, and time (Jenny, 1941). Results suggest that paleotopography, parent material, and climate (paleohydrology) are the principal factors affecting pedogenesis on the margin of paleo Lake Olduvai. A topographic relief of ~1 m affected thickness and type of soil forming on the landscape (stacked versus cumulative soil). The location of the soil with respect to the lake and the NVC particularly affected the composition of the parent material and the development of the soil through periodic additions of pyroclastic material. Lastly, fluctuating hydrology due to increasing aridity during a ~20 ka precession cycle allowed for better soil drainage and removal of elements from the system or translocation down soil profile.

5.1. Paleoenvironment and paleocatena reconstructions

Macroscale, micromorphological, and geochemical analyses reveal a complex paleocatena formed on the lake margin of paleo

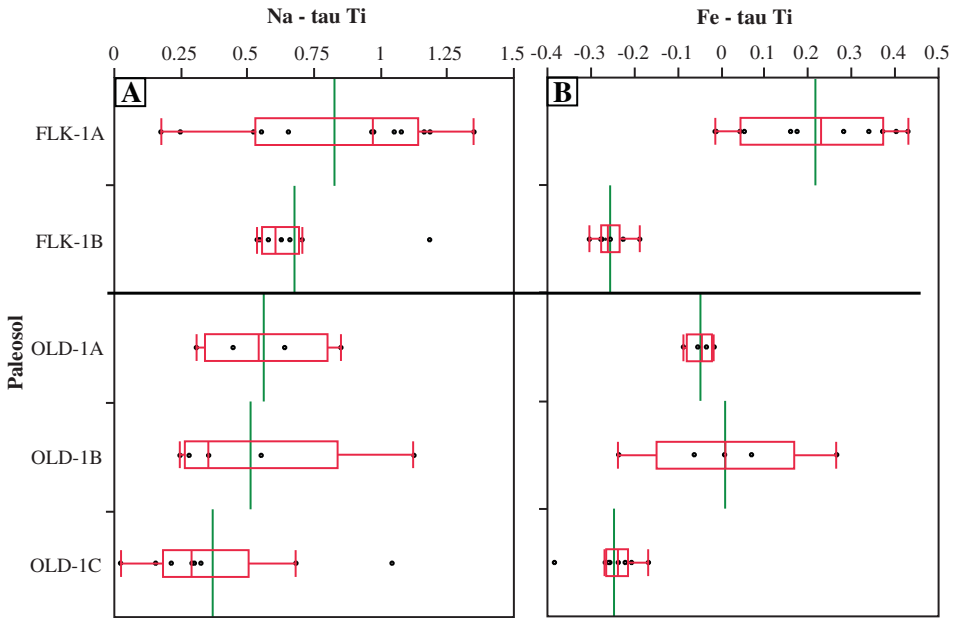

Fig. 8. Modified box plots of mass-balance calculations. (A–B) Modified box plots of Fe and Na translocation using Ti as immobile element for each paleosol. Modified box plots show the range of values, quartiles, median, and outliers. Vertical line indicates mean of each paleosol.

Lake Olduvai. Periodic expansions of the lake deposited waxy clay on the lake margin flat (Hay and Kyser, 2001; Ashley and Hay, 2002) that was then pedogenically modified during lake low stands. The abundant clay content (>80%) and vertic features identify these paleosols as weakly developed paleo-Vertisols (Blokhuis et al., 1990; Soil Survey Staff, 1999; Southard et al., 2011). Specifically, gilgai topography (Fig. 4B), abundant pedogenic slickensides identified in the field, and ubiquitous stress cutans (Fig. 5A, D, E, and G) are indicative of the shrink-swell behavior that dominates Vertisol formation (Blokhuis et al., 1990; Retallack, 2001). The vertic features are caused by precipitation seasonality with distinct wet and dry seasons that cause the soil to shrink and swell annually. These paleo-Vertisols also have distinct horizons defined by color changes (Figs. 3 and 4A), differing ped shapes and rhizoliths (Fig. 3), and element translocations (Fig. 7A–I).

The heterogeneous nature of the paleocatena is evident in thickness changes, range of vertic feature development, amount of pyroclastic contribution, organic content, and mass-bass translocations. Closest to the wetland created by the freshwater spring flowing from Zinj fault, paleosol OLD-3A shows the least amount of pedogenesis. The stress cutans surrounding the pyroclastic material are very weakly developed compared to paleosols elsewhere in the time-slice (Fig. 5A). No matrix fabric was apparent in thin section and mass-balance calculations also show evidence for less pedogenesis (Beverly, 2012). It is possible the site had slightly higher relief as it is very close to the edge of the Zinj Fault (Fig. 1C; Ashley et al., 2010a; Barboni et al., 2010; Ashley et al., 2014b). The topographic difference may be the reason for only one paleosol developing at this site.

On the footwall block of the Zinj Fault, both Trenches FLK-1 and OLD-1 contain stacked paleosols (Fig. 1C). These paleosols are separated by either tuff or tufa and are more developed than the paleosol identified in Trench OLD-3 (Fig. 3). This development is evidenced at the macroscale by more complex ped structures (Fig. 3), gilgai (Fig. 4B), and multiple types of minerals precipitating in root traces (Figs. 3, 4C and D). The micromorphology indicates greater pedogenesis with sesquans developing along irregular blocky micro-ped boundaries and better-developed soil matrix fabrics (Fig 5D). Organic matter is also more abundant in paleosols identified in Trenches OLD-1 and FLK-1 (Fig. 5B), which are closer to springs, and presumably associated wetlands depositing tufa during this time-slice (Ashley et al., 2010a), than in the paleosol in Trench OLD-2 (Fig. 5C). Phytolith and pollen records indicate that FLK region was similar to a groundwater forest where greater amounts of organic matter would accumulate than Trench OLD-2 almost 1 km from the spring that has a strong grass signature (Barboni et al., 2010).

Paleosol OLD-2A, which is located almost 1 km from the lake, formed a cumulative paleosol interval that has evidence for a greater abundance of pyroclastic material throughout the paleosol and has the best developed pedogenic microstructures. The parent material cross-plots best demonstrate this (Fig. 6A and B). Paleosol OLD-2A (solid diamonds) is significantly different from the Loc. 80 lake clay (gray squares) chosen to represent the composition of the parent material. The paleosol more closely matches the composition of the discontinuous tuff below the paleosol (open triangle). This site on the paleocatena is closest to the NVC and the pyroclastic alluvial fan to the southeast and is therefore most likely to have had a steady and increased contribution of pyroclastic material (Fig. 2).

The matrix fabric is more developed than in paleo-Vertisols closer to the lake with highly birefringent clay oriented within the matrix and surrounding grains and FeMn oxides, indicative of shrink-swell behavior of Vertisols (Fig. 5D vs 5E). Enrichment of sesquioxides (sesquans) also formed along ped boundaries and pyroclastic material (Fig. 5H). Pedorelicts (reworked clasts from older soils) are a feature unique to paleosol OLD-2A but are found only in the lower horizons of the paleosol: Bss3 and Bw3 (Fig. 5G). Pedorelicts were also identified at the top of the red paleo-Andisols intervals forming on the alluvial fan in lowermost Bed II (Ashley and Driese, 2000), and were interpreted as a period of instability that eroded soils. The pedorelicts in paleosol OLD-2A occur within the lower two horizons and support the interpretation of the paleosol as a cumulative interval with additional lake clay depositing on the soil surface and welding to the underlying soil.

In conclusion, the ~1 km cross-section of this time-slice has a small topographic relief of ~1 m that affected thickness, number,

and vertic development of paleosols on the landscape (Fig. 9A). This diagrammatic reconstruction combines field observations, micromorphological features, and geochemistry of paleosols (this study) with previous observations of faults (Hay, 1976), freshwater springs (i.e. tufa) (Ashley et al., 2010a, 2010b, 2010c), thickness of Tuff IF in the FLK locality (Hay, 1976; Ashley et al., 2010a), and vegetation based on phytoliths and pollen (Bonnefille, 1984; Barboni et al., 2010). Location on the landscape with respect to paleo Lake Olduvai, the NVC, and fault-controlled springs affected composition of the parent material, development of the soil, and organic matter content. Nearest to fault-controlled spring, pedogenesis was weakest. On the downthrown side, multiple stacked paleosols with stronger matrix fabrics, multiple ped structures, and greater organic matter preservation developed near fault-controlled springs and the associated wetlands. Closest to the NVC and volcaniclastic alluvial fan, the paleosol is cumulative with stronger matrix fabrics, sesquioxide enrichment, and pedorelicts.

These results also expand the understanding of a basin-wide paleocatena where previously two other soil-forming environments were identified (Fig. 9B). On the fluvial plain to the west of paleo Lake Olduvai, calcium carbonate-rich Aridisols formed in the well-drained quartzofeldspathic fluvial environment (Sikes and Ashley, 2007). On the lake margin, Vertisols (this study) formed on the smectite-rich lake clay where the sediment was subjected to wetting and drying due to the fluctuating lake level and seasonal monsoons. On the volcaniclastic fan to the east, red Andisols formed as a result of episodic volcaniclastic input and redoximorphic reactions associated with fluctuation of the water table (Ashley and Driese, 2000). The basin-wide catena is further summarized in Ashley et al. (2014a).

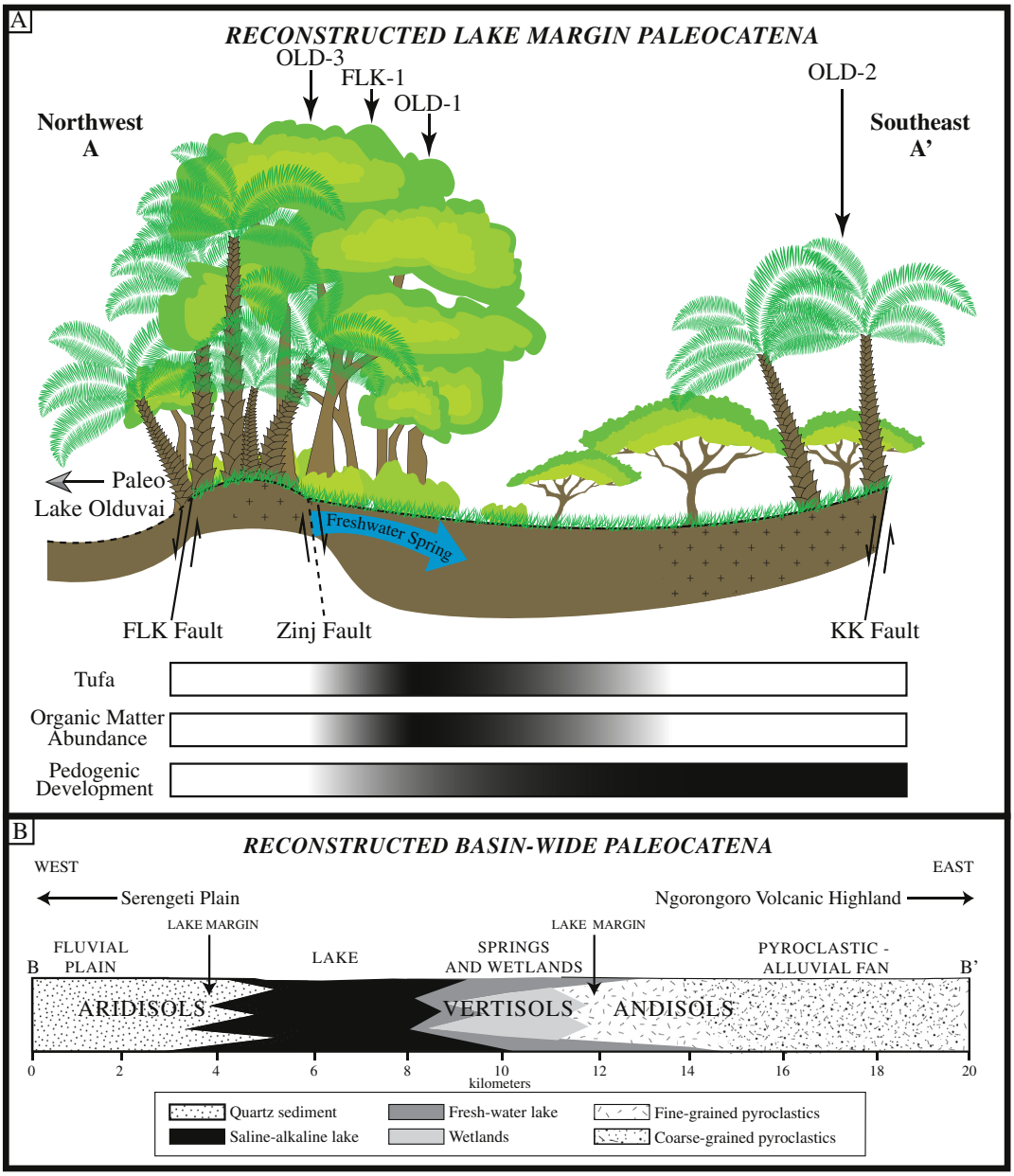

Fig. 9. Diagrammatic reconstruction of the paleolandscapes. See Fig. 3 for location on the landscape. (A) Reconstruction of the lake margin paleocatena. (B) Basin-wide reconstruction of uppermost Bed I and lowermost Bed II at ~1.8 Ma showing facies changes, interpreted depositional environments, and soil types forming on the landscape. Modified from Ashley (2000).

5.2. Paleoclimate

Previous research has demonstrated that during the Pleistocene, East African climate was primarily influenced by orbitally induced changes in insolation rather than high latitude glaciation (Trauth et al., 2009). Sapropels from northeast Africa (Tuenter et al., 2003) and East African lakes (Trauth et al., 2007) suggest that precession is the dominant driver of climate near the equator. Previous research also demonstrates ~20 ka precession cycles heavily influenced paleo Lake Olduvai between 1.84 and 1.74 Ma. Cycles of deposition of lake clay indicate that the last ~20 ka of uppermost Bed I are increasingly arid due to the decrease in rainfall associated with the dry phase of the precession cycle (Ashley, 2007). Stable isotope, faunal, floral, and lithostratigraphic records from uppermost Bed I also indicate a dry phase (Bonnefille, 1984; Cerling and Hay, 1986; Plummer and Bishop, 1994; deMenocal, 1995; Fernandez-Jalvo et al., 1998; Andrews and Humphrey, 1999; Ashley and Hay, 2002; Ashley, 2007; Bamford et al., 2008; Barboni et al., 2010).

Recent paleoclimate research using paleosols has focused on mean annual precipitation (MAP) using proxies such as CIA-K (Maynard, 1992; Sheldon et al., 2002) or Vertisol-specific proxies such as CALMAG (Nordt and Driese, 2010). The CALMAG method proved inappropriate for the Olduvai Gorge paleo-Vertisols because of the unusual chemistry of the volcanically influenced parent material. In their calculations, Nordt and Driese (2010) report values of <4% CaO and <3% MgO for Vertisols used to develop the CALMAG proxy. Olduvai paleosols contain less CaO (from 0.5% to 2%) and significantly greater amounts of MgO, ranging from 7% to as high as 17% MgO in some cases. The high Mg content is attributed to the characteristic Mg-rich smectites that formed in paleo Lake Olduvai weathering environments (Hay and Kyser, 2001; Hover and Ashley, 2003; Deocampo et al., 2009) in which these paleo-Vertisols formed, and the MgO-rich lavas erupting from Olmoti and Ngorongoro (Mollel, 2007; McHenry, 2009; Mollel et al., 2009). These lavas can range from 3 to 11% MgO, and therefore other methods were applied to understand changes in climate.

By looking at changes through time, mass-balance calculations demonstrate evidence for increasing aridity and fluctuating hydrology in the stacked paleosols from Trenches OLD-1 and FLK-1 that cannot be explained by other soil-forming factors (i.e. parent material and topography). The mass-balance calculations show an important aspect of these paleo-Vertisols not clearly identifiable through physical characteristics at the macro or petrographic scale. This is likely due to the overall weak development of the paleosols. This record would have been missed without the addition of high-resolution geochemical analyses to field and detailed petrographic description.

The oldest paleo-Vertisols FLK-1B and OLD-1C have little variability down profile in clay/zeolite accumulation or redox-responsive elements (Fig. 7A, B, D, and E). The upper paleosols generally show more variability, greater translocations (both positive and negative), and profiles more similar to a depletion–enrichment profile although most are weakly developed (Fig. 8). However, in one upper paleosol (OLD-1B) a fragipan (Figs. 3 and 4A) was identified in the field where significant translocation and accumulation occurred (Fig. 7D). The depletion of redox-responsive elements in the lower paleosols (FLK-1B and OLD-1C) is almost uniformly consistent with depth. This was probably due to longer periods of saturation with a high water table. Saturation enhanced mobility rather than translocation of soluble elements as is traditional in pedogenesis. As the climate became more arid during the precession cycle that spans the last ~20 ka of uppermost Bed I, the water table dropped allowing for increased weathering and removal of elements in a pedogenic pattern in the younger paleosols (FLK-1A, OLD-1A, OLD-1B).

The Mn profile is inconsistent with other redox-responsive elements throughout the paleosols. The variability may be due to concentration of these elements in minerals that are not distributed evenly. Mn is heavily concentrated in root traces (Fig. 4C), and the Mn translocations are indicative of concentrations of FeMn oxide precipitating around root pores. In some horizons, these root traces are concentrated in layers representative of the entire paleosol, but are also found in laterally uneven distributions that may contribute to some of the irregularity in the Mn signal.

In addition, stable isotopes of tufa have evidence for fractionation due to evaporation (Ashley et al., 2010b; Baluyot, 2011). With no evaporation and little seasonal temperature variation (~25 °C), calcite precipitated at Olduvai Gorge will have a $\delta^{18}O$ signature of approximately −6‰ (Liutkus et al., 2005). Tufa lower in the section in both FLK-1 and OLD-1 sites have calcite with $\delta^{18}O$ values between −4 and −6‰, which is evidence for precipitation of calcite with little prior evaporation. Up section, the tufa has more evolved (less negative) signature, especially in the FLK-1 samples. This suggests that the evaporation caused fractionation, and in combination with the geochemical data suggests an increasing aridity caused by the dry phase of a precession cycle.

Although mass-balance calculations indicate a drying climate, paleo Lake Olduvai continued to flood the lake margin periodically depositing Mg-rich smectites that were then pedogenically modified despite the drying phase of the precession cycle. Frequent flooding is typical of broad, shallow playas such as paleo Lake Olduvai, and small changes in MAP can create substantial variation in lake area. This scenario allows for cumulative deposition of clay and concomitant pedogenesis and is likely caused by sub-Milankovitch climate cycles. Generally the resolution of the sedimentary record at Olduvai Gorge is not sufficient to resolve millennial or smaller climate history during the Pleistocene. Resolution of late Holocene climate records in Africa on the order of decades (El Niño), centuries (Medieval Warm Period and Little Ice Age), and millennia (African Humid Period) has been successful (Gasse, 2000; Verschuren et al., 2000; Renssen et al., 2003; Driese et al., 2004; Russell and Johnson, 2007; Gasse et al., 2008; Tierney et al., 2011). Evidence suggests that these climate events had a profound effect on precipitation of Africa, and it is likely that similar climate oscillations were present in the past. Stable isotope analysis of lake margin rhizoliths suggest that these sub-Milankovitch cycles are likely responsible for the variation $\delta^{18}O$ signature of rhizoliths in cross-section (Liutkus et al., 2005).

Additional evidence for changing climatic conditions possibly due to sub-Milankovitch oscillations can be seen in the micromorphology of these paleo-Vertisols although timing of these features is not clear. A number of the paleosols in Trenches OLD-1 and OLD-2 have evidence for complex soil moisture conditions that led to authigenic precipitation in root voids and altering lapilli. FeMn oxides precipitated as rhizoliths in paleosols OLD-1B, OLD-1C, and OLD-2A. These rhizoliths are found throughout these paleosols and also concentrated in layers that are interpreted as root mats (Figs. 3 and 4C). In paleosol OLD-2A there are two distinct levels of root concentrations that provide additional evidence for the cumulative nature of the paleosol (Fig. 3). Roots and their associated microbial population often affect Fe and Mn surrounding them due to the production of organic compounds (Schwertmann and Taylor, 1989; Violante et al., 2003). Mn accumulations are often associated with a silt- or clay-rich poorly drained soil (but not extremely wet soil), which has alternating reducing and oxidizing conditions (Birnie and Paterson, 1991; Kampf et al., 2000; Stiles et al., 2001; Kraus and Hasiotis, 2006). Mn likely became mobile when the water

table was higher and the soil was poorly drained, and then roots promoted precipitation of Mn oxides in these paleo-Vertisols.

Zeolites are also found throughout the Olduvai basin in a variety of paleoenvironments (Hay, 1963, 1976; Ashley and Driese, 2000; Hay and Kyser, 2001; Mees et al., 2005; McHenry, 2009, 2010). This is primarily related to the interaction between volcanic material and the saline–alkaline lake or soil water (Mees et al., 2005). Zeolites are observed altering lapilli and precipitating in root voids in all sites within the time-slice. Paleosol OLD-3A is closest to the lake and contains the largest number of zeolitized lapilli, and thus presumably more influenced by saline–alkaline lake water (Fig. 5A). In Trenches OLD-1 and FLK-1 where the paleosols are stacked, zeolites are only found in the lower paleosols (FLK-1B, OLD-1B, and OLD-1C). In the case of paleosols FLK-1B and OLD-1C, zeolitized root traces also coincide with the appearance of lapilli (Fig. 3). In Trench OLD-2 where the paleosols are cumulative, the zeolites are also found at the base of the profile where there are also lapilli (Figs. 3 and 4D). The occurrence of these zeolites seems connected to the amount of pyroclastic material available and depth in the soil profile.

This geochemical system shows similarities with Lake Bogoria where zeolites precipitated during prolonged dry periods (Renaut, 1993; Owen et al., 2009). Zeolitic rhizoliths are rare and probably only precipitate in dry, saline–alkaline soils where saline–alkaline fluids are available. These types of rhizoliths are usually a result of a significant period of aridity where capillary rise and evaporative pumping drew up saline–alkaline water (Owen et al., 2009). A similar system likely formed on the margin of paleo Lake Olduvai where abundant volcaniclastic material interacted with saline–alkaline water drawn upwards during the drying trend in uppermost Bed I.

In paleosol OLD-2A, there is also evidence for the relative timing of the precipitation of the Mn oxides and zeolites. Root voids were first lined with Mn oxides and then zeolite crystals (Fig. 5F). Ashley and Driese (2000) note a similar but better developed record with a relative sequence of formation of pedogenic features in lowermost Bed II. The paleohydrology of this red paleosol interval was recorded in 1) redoximorphic features, 2) illuviated clay coatings, 3) a second generation of redoximorphic features, 4) vadose silt, and 5) zeolite pore-fillings and alteration of volcanic glass. The redoximorphic features are interpreted to be associated with fluctuating higher water table and wetter climate that impeded soil drainage. The illuviated clay coatings indicated a slightly drier climate, and the vadose silt was evidence of a much drier climate. The zeolites were interpreted to be associated with the interaction between the soil and the saline–alkaline lake.

6. Conclusions

Paleosols in the upper Bed I time-slice formed from a lake clay parent material deposited during expansions of Lake Olduvai over a ~20 ka time-slice at ~1.8 Ma and recorded a paleocatena. The field relationships, macroscale and petrographic features, and mass-balance calculations all identify these paleosols as weakly developed paleo-Vertisols. The paleohydrology, paleotopography, and periodic additions of pyroclastic material resulted in a heterogeneous paleocatena along the eastern margin of paleo Lake Olduvai. In this NW–SE trending transect, the soil was poorly developed near the lake margin while stacked soils developed in the accommodation space created by faulting, and cumulative soils developed closer to the volcaniclastic alluvial fan (Fig. 9A). These results also identify a soil-forming environment (previously undescribed) that contributes to the understanding of the paleolandscape within the Olduvai Basin. Differences in topography, depositional environment, parent material, and depth to the water table are reflected in the development of different soil types across the landscape (Fig. 9B).

The abundance of vertic features identified in outcrop and in the micromorphology in these paleo-Vertisols indicates monsoonal precipitation during this time-slice. The bulk geochemistry of the paleo-Vertisols also reveals a fluctuating hydrology not clearly visible in outcrop or the micromorphology. The mass balance calculations of the stacked paleo-Vertisols at FLK-1 and OLD-1 indicate greater translocations (positive and negative) between 1.79 and 1.81 Ma. A lower water table due to decreased precipitation would allow for better drainage and therefore increased pedogenesis. This trend is likely due to the effects of a precession cycle and correlates well with existing faunal, floral, and lithostratigraphic records at Olduvai Gorge, as well as dust and oxygen isotope records from marine cores in Africa.

Sub-Milankovitch cycles are also identified in the paleo-Vertisols using the micromorphology. Multiple authigenic minerals precipitated in rhizoliths likely due to changing hydrology from decreased precipitation. Redox-sensitive Mn was mobilized during saturated soil conditions and precipitated during drier conditions. Zeolites altering lapilli and precipitating in root traces are a result of drying climate causing capillary rise and evaporative pumping of saline–alkaline water upward. In most areas on the paleocatena, these authigenic minerals do not precipitate within the same paleosol. In the paleo-Vertisol furthest from paleo Lake Olduvai, cross-cutting relationships show that root voids were first lined with FeMn oxides followed by zeolite crystals (Fig. 5F). Timing of these features is not clear but suggests that wetter and drier periods existed within the precession cycle identified in this 20 ka time-slice at 1.8 Ma.

This time-slice also contains one of the densest concentrations of artifacts and large mammal bones materials found at Olduvai Gorge and coincides with the first hominin migrations out of Africa ~1.8 Ma. The additional data provided by the paleo-Vertisols in uppermost Bed I suggest that hominins living at Olduvai Gorge faced a water-stressed environment with annual precipitation seasonality, sub-Milankovitch cycles (i.e. El Niño, the Little Ice Age, or the African Humid Period), and precession cycles. The additional evidence for inconsistent precipitation found in the paleo-Vertisols and lack of potable water from paleo Lake Olduvai add credence to the argument that the freshwater springs attracted both carnivores and humans.

Acknowledgements

The data presented here were collected under permits from the Tanzanian Commission for Science and Technology and the Tanzanian Antiquities Department to The Olduvai Paleoanthropology and Paleoecology Project (TOPPP), PIs M. Domínguez-Rodrigo, A.Z.P. Mabulla, H.T. Bunn, and E. Baquedano. We greatly appreciate funding from the Evolving Earth Foundation, Rutgers University Department of Earth and Planetary Sciences, and Geological Society of America Student Research Grant. We are grateful for the hospitality of members of the TOPPP research team while conducting research in Tanzania and for the help of T. Ombori and B. Mbasa from the University of Dar es Salaam.

References

Andrews, P., Humphrey, L., 1999. African Miocene environments and transition to early Hominines. In: Bromage, T.G., Schrenk, F. (Eds.), African Biogeography, Climate Change, and Human Evolution. Oxford University Press, New York, pp. 282–303.

Ashley, G., Tactikos, J., Owen, R., 2009. Hominin use of springs and wetlands: paleoclimate and archaeological records from Olduvai Gorge (~1.79–1.74 Ma). Palaeogeography, Palaeoclimatology, Palaeoecology 272, 1–16.

Ashley, G.M., 2000. Geologists probe hominid environments. GSA Today 10, 24–29.
Ashley, G.M., 2007. Orbital rhythms, monsoons, and playa lake response, Olduvai Basin, equatorial East Africa (ca. 1.85–1.74 Ma). Geology 35, 1091–1094.
Ashley, G.M., Barboni, D., Domínguez-Rodrigo, M., Bunn, H.T., Mabulla, A.Z.P., Diez-Martin, F., Barba, R., Baquedano, E., 2010a. Paleoenvironmental and paleoecological reconstruction of a freshwater oasis in savannah grassland at FLK North, Olduvai Gorge, Tanzania. Quaternary Research 74, 333–343.
Ashley, G.M., Barboni, D., Domínguez-Rodrigo, M., Bunn, H.T., Mabulla, A.Z.P., Diez-Martin, F., Barba, R., Baquedano, E., 2010b. A spring and wooded habitat at FLK Zinj and their relevance to origins of human behavior. Quaternary Research 74, 304–314.
Ashley, G.M., Domínguez-Rodrigo, M., Bunn, H.T., Mabulla, A.Z.P., Baquedano, E., 2010c. Sedimentary geology and human origins: a fresh look at Olduvai Gorge, Tanzania. Journal of Sedimentary Research 80, 703–709. http://dx.doi.org/10.2110/jsr.2010.066.
Ashley, G.M., Beverly, E.J., Sikes, N.E., Driese, S.G., 2014a. Paleosol diversity in the Olduvai Basin, Tanzania, effects of geomorphology, parent material, depositional environment, and groundwater on soil development. Quaternary International 322-323, 66–77.
Ashley, G.M., Bunn, H.T., Delaney, J.S., Barboni, D., Domínguez-Rodrigo, M., Mabulla, A.Z.P., Gurtov, A.N., Baluyot, R., Beverly, E.J., Baquedano, E., 2014b. Paleoclimatic and paleoenvironmental framework of FLK North archaeological site, Olduvai Gorge, Tanzania. Quaternary International 322-323, 54–65.
Ashley, G.M., Deocampo, D.M., Kahmann-Robinson, J.A., Driese, S.G., 2013c. Groundwater-fed wetland sediments and paleosols: It's all about water table. In: Driese, Steven G., Nordt, L.C. (Eds.), New Frontiers in Paleopedology and Terrestrial Paleoclimatology, SEPM Special Publication No. 104: New Frontiers in Paleopedology and Terrestrial Paleoclimatology. SEPM, Tulsa, pp. 47–62.
Ashley, G.M., Driese, S.G., 2000. Paleopedology and paleohydrology of a volcaniclastic paleosol interval: Implications for Early Pleistocene stratigraphy and paleoclimate record: Olduvai Gorge, Tanzania. Journal of Sedimentary Research 70, 1065–1080.
Ashley, G.M., Hay, R.L., 2002. Sedimentation patterns in a Plio-Pleistocene volcaniclastic rift-platform basin, Olduvai Gorge, Tanzania. In: Renaut, R.W., Ashley, G.M. (Eds.), Sedimentation in Continental Rifts. SEPM Special Publications, pp. 107–122.
Baluyot, R., 2011. Paleoenvironmental reconstruction of a Pleistocene landscape, Olduvai Gorge, Tanzania. Earth and Planetary Sciences, 46. Rutgers University.
Bamford, M.K., Stanistreet, I.G., Stollhofen, H., Albert, R.M., 2008. Late Pliocene grassland from Olduvai Gorge, Tanzania. Palaeogeography, Palaeoclimatology, Palaeoecology 257, 280–293.
Barboni, D., Ashley, G.M., Domínguez-Rodrigo, M., Bunn, H.T., Mabulla, A., Baquedano, E., 2010. Phytoliths infer dense and heterogeneous paleovegetation at FLK North and surrounding localities during upper Bed I time, Olduvai Gorge, Tanzania. Quaternary Research 74, 344–354.
Berggren, W.A., Kent, D.V., Swisher, C.C., Aubry, M.-P., 1995. A revised Cenozoic geochronology and chronostratigraphy. In: Geochronology, Time Scales and Global Stratigraphic Correlation. Society of Economic Paleontologists and Mineralogists Special Publication, vol. 54, pp. 129–212.
Beverly, E.J., 2012. Paleoenvironmental and Paleoclimatic Reconstruction of a Pleistocene Catena Using Paleopedology and Geochemistry of Lake Marigin Paleo-Vertisols, Olduvai Gorge, Tanzania. Department of Geological Sciences, Rutgers University, New Brunswick, p. 103. http://hdl.rutgers.edu/1782.1/rucore10001600001.ETD.000063988.
Birnie, A.C., Paterson, E., 1991. The mineralogy and morphology of iron and manganese oxides in an imperfectly drained Scottish soil. Geoderma 50, 219–237.
Blake, G.R., Hartge, K.H., 1986. Bulk density. In: Klute, A. (Ed.), Methods of Soil Analysis: Part I Physical and Mineralogical Methods. Soil Science Society of America, Inc., Madison, pp. 363–375.
Blokhuis, W.A., Kooistra, M.J., Wilding, L.P., 1990. Micromorphology of cracking clayey soils (vertisols). In: Douglas, L.A. (Ed.), Soil Micromorphology: a Basic and Applied Science. Elsevier, New York.
Bonnefille, R., 1984. Palynological Research at Olduvai Gorge. National Geographic Society Research Reports. National Geographic Society, pp. 227–243.
Brantley, S.L., Goldhaber, M.B., Ragnarsdottir, K.V., 2007. Crossing disciplines and scales to understand the Critical Zone. Elements 3, 307–314.
Brewer, R., 1976. Fabric and Mineral Analysis of Soils. John Wiley & Sons, Inc., New York, p. 470.
Brimhall, G.H., Chadwick, O.A., Lewis, C.J., Compston, W., Williams, I.S., Danti, K.J., Dietrich, W.E., Power, M.E., Hendricks, D., Bratt, J., Wiliams, I.S., 1991a. Deformational mass in invasive processes transport and soil evolution. Science 255, 695–702.
Brimhall, G.H., Dietrich, W.E., 1987. Constitutive mass balance relations between chemical composition, volume, density, porosity, and strain in metasomatic hydrochemical systems: results on weathering and pedogenesis. Geochimica et Cosmochimica Acta 51, 567–587.
Brimhall, G.H., Lewis, C.J., Ford, C., Bratt, J., Taylor, G., Warin, O., 1991b. Quantitative geochemical approach to pedogenesis: importance of parent material reduction, volumetric expansion, and eolian influx in lateritization. Geoderma 51, 51–91.
Bunn, H.T., Mabulla, A., Domínguez-Rodrigo, M., Ashley, G., Barba, R., Diez-Martin, F., Remer, K., Yravedra, J., Baquedano, E., 2010. Was FLK North levels 1-2 a classic "living floor" of Oldowan hominids or a taphonomically complex palimpsest dominated by large carnivore feeding behavior? Quaternary Research 74, 355–362.
Cerling, T.E., Hay, R.L., 1986. An isotopic study of paleosol carbonates from Olduvai Gorge. Quaternary Research 25, 63–78.
Chadwick, O.A., Brimhall, G.H., Hendricks, D.M., 1990. From a black to a gray box – a mass balance interpretation of pedogenesis. Geomorphology 3, 369–390.
Deino, A.L., 2012. (40)Ar/(39)Ar dating of Bed I, Olduvai Gorge, Tanzania, and the chronology of early Pleistocene climate change. Journal of Human Evolution 63, 251–273.
deMenocal, P.B., 1995. Plio-Pleistocene African climate. Science 270, 53–59.
Deocampo, D.M., Blumenschine, R.J., Ashley, G.M., 2002. Wetland diagenesis and traces of early hominids, Olduvai Gorge, Tanzania. Quaternary Research 57, 271–281.
Deocampo, D.M., Cuadros, J., Wing-Dudek, T., Olives, J., Amouric, M., 2009. Saline lake diagenesis as revealed by a coupled mineralogy and geochemistry of multiple ultrafine clay phases: Pliocene Olduvai Gorge, Tanzania. American Journal of Science 309, 834–868.
Domínguez-Rodrigo, M., Barba, R., Egelund, C.P., 2007. Deconstructing Olduvai: a Taphonomic Study of Bed I Sites. In: Vertebrate Paleobiology and Paleoanthropology Series. Springer, Dordrecht, pp. 127–164.
Domínguez-Rodrigo, M., Mabulla, A., Bunn, H.T., Diez-Martin, F., Baquedano, E., Barboni, D., Barba, R., Dominguez-Solera, S., Sanchez, P., Ashley, G.M., Yravedra, J., 2010. Disentangling hominin and carnivore activities near a spring at FLK North (Olduvai Gorge, Tanzania). Quaternary Research 74, 363–375.
Driese, S.G., Ashley, G.M., Li, Z.-H., Hover, V.C., Owen, R.B., 2004. Possible Late Holocene equatorial palaeoclimate record based upon soils spanning the Medieval Warm Period and Little Ice Age, Loboi Plain, Kenya. Palaeogeography, Palaeoclimatology, Palaeoecology 213, 231–250.
Driese, S.G., Mora, C.I., Stiles, C.A., Joeckel, R.M., Nordt, L.C., 2000. Mass-balance reconstruction of a modern Vertisol: implications for interpreting the geochemistry and burial alteration of paleo-Vertisols. Geoderma 95, 179–204.
Feakins, S.J., deMenocal, P.B., 2010. Global and African regional climate change during the Cenozoic. In: Werdelin, L., Sanders, W.J. (Eds.), Cenozoic Mammals of Africa. University of California Press, pp. 45–55.
Fernandez-Jalvo, Y., Denys, C., Andrews, P., Williams, T., Dauphin, Y., Humphrey, L., 1998. Taphonomy and palaeoecology of Olduvai Bed-I (Pleistocene, Tanzania). Journal of Human Evolution 34, 137–172.
Ferring, R., Oms, O., Agustí, J., Berna, F., Nioradze, M., Shelia, T., Tappen, M., Vekua, A., Zhvania, D., Lordkipanidze, D., 2011. Earliest human occupations at Dmanisi (Georgian Caucasus) dated to 1.85–1.78 Ma. Proceedings of the National Academy of Sciences of the United States of America 108, 1–5.
Fitzpatrick, E.A., 1993. Soil Microscopy and Micromorphology. John Wiley & Sons, New York, p. 304.
Gabunia, L., Vekua, A., Lordkipanidze, D., Swisher III, C.C., Ferring, R., Justus, A., Nioradze, M., Tvalchrelidze, M., Anton, S.C., Bosiniski, G., Joris, O., De Lumley, M.A., Majsuradze, G., Mouskhelishvili, A., 2000. Earliest Pleistocene hominid cranial remains from Dmanisi, Republic of Georgia: Taxonomy, geologic setting, and age. Science 288.
Gasse, F., 2000. Hydrological changes in the African tropics since the Last Glacial Maximum. Quaternary Science Reviews 19, 189–211.
Gasse, F., Chalié, F., Vincens, A., Williams, M.A.J., Williamson, D., 2008. Climatic patterns in equatorial and southern Africa from 30,000 to 10,000 years ago reconstructed from terrestrial and near-shore proxy data. Quaternary Science Reviews 27, 2316–2340.
Gromme, C.S., Hay, R.L., 1971. Geomagnetic polarity epochs: age and duration of the Olduvai normal polarity event. Earth and Planetary Science Letters 10, 179–185.
Hay, R.L., 1963. Zeolitic weathering in Olduvai Gorge, Tanganyika. Geological Society of America Bulletin 74, 1281–1286.
Hay, R.L., 1976. Geology of the Olduvai Gorge: a Study of Sedimentation in a Semiarid Basin. University of California Press, Berkeley, p. 203.
Hay, R.L., 1992. Potassium-argon dating of Bed I, Olduvai Gorge, 1961–1972. Quaternary International 13–14, 31–36.
Hay, R.L., Kyser, T.K., 2001. Chemical sedimentology and paleoenvironmental history of Lake Olduvai, a Pliocene lake in northern Tanzania. GSA Bulletin 113, 1505–1521.
Hover, V.C., Ashley, G.M., 2003. Geochemical signatures of paleodepositional and diagenetic environments: a STEM/AEM study of authigenic clay minerals from an arid rift basin, Olduvai Gorge, Tanzania. Clays and Clay Minerals 51, 231–251.
Jenny, H., 1941. Factors of Soil Formation: a System of Quantitative Pedology. McGraw-Hill, New York, p. 288.
Kampf, N., Scheinost, A.C., Schulze, D.G., 2000. Oxide minerals. In: Sumner, M.E. (Ed.), Handbook of Soil Sciences. CRC Press, Boca Raton, Florida, pp. F125–F168.
Kappelman, J., 1986. Plio-Pleistocene marine-continental correlation using habitat indicators from Olduvai Gorge, Tanzania. Quaternary Research 25, 141–149.
Klaus, K.E., Neuendorf Jr., J.P., Jackson, J.A., 2005. Glossary of Geology. American Geological Institute, Alexandria, VA, p. 800.
Kraus, M.J., Hasiotis, S.T., 2006. Significance of different modes of rhizolith preservation to interpreting paleoenvironmental and paleohydrologic settings: examples from Paleogene paleosols, Bighorn Basin, Wyoming, U.S.A. Journal of Sedimentary Research 76, 633–646.
Kutzbach, J.E., Liu, Z., 1997. Response of the African monsoon to orbital forcing and ocean feedbacks in the middle Holocene. Science 278, 440–443.
Leakey, M.D., 1971. Olduvai Gorge: Excavations in Beds I and II, 1960–1963. Cambridge University Press, Cambridge, p. 309.
Liutkus, C.M., Wright, J.D., Ashley, G.M., Sikes, N.E., 2005. Paleoenvironmental interpretation of lake-margin deposits using $\delta^{13}C$ and $\delta^{18}O$ results from early Pleistocene carbonate rhizoliths, Olduvai Gorge, Tanzania. Geology 33, 377.

Lordkipanidze, D., Jashashvili, T., Vekua, A., Ponce de Leon, M.S., Zollikofer, C.P., Rightmire, G.P., Pontzer, H., Ferring, R., Oms, O., Tappen, M., Bukhsianidze, M., Agusti, J., Kahlke, R., Kiladze, G., Martinez-Navarro, B., Mouskhelishvili, A., Nioradze, M., Rook, L., 2007. Postcranial evidence from early Homo from Dmanisi, Georgia. Nature 449, 305–310.

Magill, C.R., Ashley, G.M., Freeman, K.H., 2012a. Feature article: ecosystem variability and early human habitats in eastern Africa. Proceedings of the National Academy of Sciences of the United States of America 662, 1–8.

Magill, C.R., Ashley, G.M., Freeman, K.H., 2012b. Feature article: water, plants, and early human habitats in eastern Africa. Proceedings of the National Academy of Sciences of the United States of America 80, 1–6.

Maynard, J.B., 1992. Chemistry of modern soils as a guide to interpreting precambrian paleosols. Journal of Geology 100, 279–289.

McHenry, L., 2004. Characterization and correlation of altered Plio-Pleistocene tephra using a "multiple technique" approach: case study at Olduvai Gorge, Tanzania. Earth and Planetary Sciences, 382. Rutgers University.

McHenry, L., 2005. Phenocryst composition as a toll for correlating fresh and altered tephra, Bed I, Olduvai Gorge, Tanzania. Stratigraphy 2, 101–115.

McHenry, L.J., 2009. Element mobility during zeolitic and argillic alteration of volcanic ash in a closed-basin lacustrine environment: case study Olduvai Gorge, Tanzania. Chemical Geology 265, 540–552.

McHenry, L.J., 2010. Element distribution between coexisting authigenic mineral phases in argillic and zeolitic altered tephra, Olduvai Gorge, Tanzania. Clays and Clay Minerals 58, 627–643.

Mees, F., Stoops, G., Van Ranst, E., Paepe, R., Van Overloop, E., 2005. The nature of zeolite occurrences in deposits of the Olduvai Basin, Northern Tanzania. Clays and Clay Minerals 53, 659–673.

Mollel, G.F., 2007. Petrochemistry and Geochronology of Ngorongoro Volcanic Highland Complex (NVHC) and its Relationship to Laetoli and Olduvai Gorge, Tanzania. Department of Geology. Rutgers University.

Mollel, G.F., Swisher III, C.C., McHenry, L.J., Feigenson, M.D., Carr, M.J., 2009. Petrogenesis of basalt–trachyte lavas from Olmoti Crater, Tanzania. Journal of African Earth Sciences 54, 127–143.

Nordt, L.C., Driese, S.G., 2010. New weathering index improves paleorainfall estimates from Vertisols. Geology 38, 407–410.

Nicholson, S.E., 2000. The nature of rainfall variability over Africa on time scales of decades to millenia. Global and Planetary Change 26, 137–158.

Owen, R.B., Renaut, R.W., Scott, J.J., Potts, R., Behrensmeyer, A.K., 2009. Wetland sedimentation and associated diatoms in the Pleistocene Olorgesailie Basin, southern Kenya Rift Valley. Sedimentary Geology 222, 124–137.

Plummer, T.W., Bishop, L.C., 1994. Hominid paleoecology of Olduvai Gorge, Tanzania as indicated by antelope remains. Journal of Human Evolution 27, 47–75.

Renaut, R.W., 1993. Zeolitic diagenesis of late Quaternary fluviolacustrine sediments and associated calcrete formation in the Lake Borgoria Basin, Kenyar Rift Valley. Sedimentology 40, 271–301.

Renssen, H., Brovkin, V., Fichefet, T., Goosse, H., 2003. Holocene climate instability during the termination of the African Humid Period. Geophysical Research Letters 30, 33-1–33-4.

Retallack, G.J., 2001. Soils of the Past: an Introduction to Paleopedology. Blackwell Science Ltd, Oxford, p. 512.

Ruddiman, W.F., 2008. Earth's Climate: Past and Future. W. H. Freeman and Company, New York, p. 388.

Russell, J.M., Johnson, T.C., 2007. Little Ice Age drought in equatorial Africa: intertropical convergence zone migrations and El Niño–Southern Oscillation variability. Geology 35, 21–24.

Schwertmann, U., Taylor, R.M., 1989. Iron oxides. In: Dixon, J.B., Weed, S.B. (Eds.), Minerals in Soil Environments. Soil Science Society of America, Madison, Wisconsin, pp. 379–438.

Sheldon, N.D., Retallack, G.J., Tanaka, S., 2002. Geochemical climofunctions from North America soils and applications to paleosols across the Eocene-Oligocene Boundary in Oregon. The Journal of Geology 110, 687–696.

Sheldon, N.D., Tabor, N.J., 2009. Quantitative paleoenvironmental and paleoclimatic reconstruction using paleosols. Earth-Science Reviews 95, 1–52.

Sikes, N.E., Ashley, G.M., 2007. Stable isotopes of pedogenic carbonates as indicators of paleoecology in the Plio-Pleistocene (upper Bed I), western margin of the Olduvai Basin, Tanzania. Journal of Human Evolution 53, 574–594.

Southard, R.J., Driese, S., Nordt, L., 2011. Vertisols. In: Huang, P.M., Li, Y., Sumner, M.E. (Eds.), Handbook of Soil Science, second ed. CRC Press, Boca Raton, Florida, pp. 33–97 (Chapter 33.7).

Soil Survey Staff, 1999. Vertisols. Soil Taxonomy: a Basic System of Soil Classification for Making and Interpreting Soil Surveys. In: Agriculture Handbook, vol. 436. United States Department of Agriculture, Washington D.C, pp. 783–817.

Stiles, C.A., Mora, C.I., Driese, S.G., 2001. Pedogenic iron-manganese nodules in Vertisols: a new proxy for paleoprecipitation? Geology 29, 943–946.

Stiles, C.A., Mora, C.I., Driese, S.G., 2003a. Pedogenic processes and domain boundaries in a Vertisol climosequence: evidence from titanium and zirconium distribution and morphology. Geoderma 116, 279–299.

Stiles, C.A., Mora, C.I., Driese, S.G., Robinson, A.C., 2003b. Distinguishing climate and time in the soil record: mass-balance trends in Vertisols from the Texas coastal prairie. Geology 31, 331–334.

Tamrat, E., Thouveny, N., Taieb, M., Opdyke, N.D., 1995. Revised magnetostratigraphy of the Plio–Pleistocene sedimentary sequence of the Olduvai Formation (Tanzania). Palaeogeography, Palaeoclimatology, Palaeoecology 114, 273–283.

Tierney, J.E., Lewis, S.C., Cook, B.I., LeGrande, A.N., Schmidt, G.A., 2011. Model, proxy and isotopic perspectives on the East African Humid Period. Earth and Planetary Science Letters 307, 103–112.

Trauth, M.H., Larrasoaña, J.C., Mudelsee, M., 2009. Trends, rhythms and events in Plio-Pleistocene African climate. Quaternary Science Reviews 28, 399–411.

Trauth, M.H., Maslin, M.A., Deino, A.L., Strecker, M.R., Bergner, A.G., Duhnforth, M., 2007. High- and low-latitude forcing of Plio-Pleistocene East African climate and human evolution. Journal of Human Evolution 53, 475–486.

Tuenter, E., Weber, S.L., Hilgen, F.J., Lourens, L.J., 2003. The response of the African summer monsoon to remote and local forcing due to precession and obliquity. Global and Planetary Change 36, 219–235.

Verschuren, D., Laird, K.R., Cumming, B.F., 2000. Rainfall and drought in equatorial east Africa during the past 1,100 years. Nature 403, 410–414.

Violante, A., Barberis, E., Pigna, M., Boero, V., 2003. Factors affecting the formation, nature, and properties of iron precipitation products at the soil-root interface. Journal of Plant Nutrition 26, 1889–1908.